Free-Space Optical Communications: Capacity Bounds, Approximations, and a New Sphere-Packing Perspective

This article has been accepted for publication in a future issue of this journal, but has not been fully edited. Content may change prior to final publication. Citation information: DOI 10.1109/TCOMM.2016.2524569, IEEE Transactions on Communications

Free-Space Optical Communications: Capacity Bounds, Approximations, and a New Sphere-Packing Perspective

Anas Chaaban, Jean-Marie Morvan, and Mohammad Slim Alouini

***Abstract*—The capacity of the free-space optical channel is studied. A new recursive approach for bounding the capacity of the channel based on sphere-packing is proposed. This approach leads to new capacity upper bounds for a channel with a peak intensity constraint or an average intensity constraint. Under an average constraint only, the derived bound is tighter than an existing sphere-packing bound derived earlier by Farid and Hranilovic. The achievable rate of a truncated-Gaussian input distribution is also derived. It is shown that under both average and peak constraints, this achievable rate and the sphere-packing bounds are within a small gap at high SNR, leading to a simple high-SNR capacity approximation. Simple fitting functions that capture the best known achievable rate for the channel are provided. These functions can be of practical importance especially for the study of systems operating under atmospheric turbulence and misalignment conditions.**

***Index Terms*—Intensity-modulation, sphere-packing, capacity bounds, capacity approximation, truncated-Gaussian.**

I. Introduction

Free-space optical (FSO) communication has attracted lots of research attention recently [2]–[7] due to its ability to provide high-speed communication while not being too demanding in terms of infrastructure [8], [9]. As such, it is an important solution for scenarios where deploying infrastructure is prohibitive (dangerous terrain) or not cost-effective (temporary situations). FSO is also a potential solution for the main challenge facing today's radio-frequency communication: spectrum shortage.

Although optical heterodyne detection can be employed in FSO [10], IM-DD is favored from a practical point of view due to its simplicity and low-cost. Several models exist for IM-DD channels [8], and one of the most often studied models is the Gaussian channel with input-independent Gaussian noise [11]–[16]. In this model, the input signal is a positive random variable representing the optical intensity, and the noise is input-independent Gaussian. In addition to its nonnegativity, the input signal is typically restricted by a peak and an average constraint due to safety and practical considerations [17]. Although the capacity achieving input distribution is known to be discrete [16], the capacity of the channel is yet unknown in closed-form.

Nevertheless, several bounds on the channel capacity exist, and these bounds are tight in some cases [11]–[15]. For instance, for a channel with an average constraint only, [11] derived capacity upper and lower bounds that meet at high signal-to-noise ratio (SNR). Under an average and peak intensity constraints, the upper and lower bounds in [11] meet at high and low SNR. The highest known achievable rate for the channel was given in [12], where the best discrete distribution with equally spaced mass points was found. This distribution achieves rates close to capacity as shown in [12]. On the other hand, [13] derived bounds for the channel under an average constraint only, where it was shown that the best discrete distribution with equally spaced mass points is the geometric distribution. In the same paper, an upper bound was derived by using sphere-packing in a simplex. Despite this work, a simple capacity expression is still to be found.

Our work in this paper can be considered rather complementing the work in [11], [12] for an IM-DD channel with both average and peak constraints. As in [13], we bound the capacity of the IM-DD channel using a sphere-packing approach. Under a peak constraint, we get a problem of sphere-packing in a cube. We derive upper bounds for this case using two approaches. The first approach is similar to the one used in [13] which employs the Steiner-Minkowski formula for polytopes [18]–[20]. The second approach is based on a new recursive argument that better capitalizes on the geometry of the ball, and hence yields better bounds at moderate/high SNR. For the IM-DD channel with only an average constraint, the new approach yields a significantly better bound than the one derived in [13] for any SNR. This is due to exploiting the geometry of the ball while deriving the bounds. The derived sphere-packing bounds coincide with the high SNR capacity of the channel with an average constraint only, and the channel with average and peak constraints with a dominant peak constraint, which reproduces the results of [11] for those cases. The advantage is that sphere-packing bounds have a simpler interpretation than the bounds in [11] due to their geometric nature.

In [11], continuous input distributions that achieve the high-SNR capacity of the channel were given. Continuous input distributions lead to achievable rates that can be written in simple expressions, contrary to discrete input distributions [12]. We ask the questions whether other continuous distributions

Parts of this paper have been presented in IWOW'2015 [1].

The authors are with King Abdullah University of Science and Technology (KAUST), Computer, Electrical, and Mathematical Sciences and Engineering Division (CEMSE), Thuwal 23955-6900, Saudi Arabia. Email: {anas.chaaban,jean-marie.morvan,slim.alouini}@kaust.edu.sa.

J.-M. Morvan is on leave from Université de Lyon, CNRS, Université Claude Bernard Lyon 1, ICJ UMR 5208, Villeurbanne F-69622 France.

This work is supported in part by King Abdulaziz City of Science and Technology (KACST) under grant AT-34-145 and by King Abdullah University of Science and Technology (KAUST).

This article has been accepted for publication in a future issue of this journal, but has not been fully edited. Content may change prior to final publication. Citation information: DOI 10.1109/TCOMM.2016.2524569, IEEE Transactions on Communications

than those in [11] can achieve higher rates at moderate SNR. To this end, we derive the achievable rate of a truncated-Gaussian (TG) input distribution. This answers the question in the affirmative. The expression of the achievable rate is rather complicated, and requires optimization over two parameters. We lower bound this achievable rate by a simpler expression, and provide values for the optimization parameters which yield fairly good performance at high SNR. In particular, we show that the TG distribution is nearly capacity achieving[1] at high SNR if the peak constraint dominates the average constraint. Otherwise, we show that the TG distribution achieves the sphere-packing bounds within a gap of at most 0.163 nats, although this gap can be reduced numerically to 0.1 nats. Based on this, we approximate the high-SNR capacity by the sphere-packing bounds. We note that the gap reduces to approximately zero by incorporating a bound from [11]. This leads to the conclusion that the TG distribution is nearly capacity achieving at high SNR.

The best achievable rate known to-date remains the one given in [12], which is fairly close to the upper bounds at any SNR. However, this achievable rate is derived numerically, and does not have a closed-form expression. A closed-form expression is important for the study of practical systems under fading scenarios. The availability of such an expression allows a better understanding of the ultimate performance of IM-DD systems beyond simple sub-optimal schemes such as on-off keying [2], [3], [21] or binary pulse-position modulation [22], [23], and beyond high SNR scenarios with only an average constraint [24]. To make the capacity approaching scheme in [12] more accessible, we provide a simple fitting function which closely captures its achievable rate globally (at any SNR). This expression is of the form $\frac{1}{2}\log(1+\gamma^2 f(\gamma))$ where γ is the SNR and $f(\gamma)$ is of the form $p(\gamma)/q(\gamma)$ which are both polynomials of the same degree in γ. It turns out that fixing the degrees of these polynomials to 1 provides a sufficiently good fit, while increasing it to 3 provides a very close fit at the expense of a more sophisticated expression. We also provide a simpler local fitting function of the form $\frac{d_1}{2}\log(1+d_3\gamma^2)$ which provides a close fit within a desired range of SNR.

The rest of the paper is organized as follows. The system model is given in Section II. The main results of the paper are given in Section III, and are proved in the remaining sections. In Section IV, we derive capacity upper bounds using sphere-packing in a cube. In Section V, we derive a capacity upper bound using our recursive approach on sphere-packing in a simplex. In Section VI, we derive the achievable rate using a TG distribution, and approximate the high-SNR capacity. We provide capacity fitting functions in Section VII, and we conclude in Section VIII.

Throughout the paper, we use normal-face font to denote scalars, and bold-face font to denote vectors. We use $g_{\mu,\nu}(x)$ to denote the Gaussian distribution with mean μ and variance ν^2, and $G_{\mu,\nu}(x)$ to denote its cumulative distribution function. We also use $V(\cdot)$ to denote the volume of an object. Next, we introduce the IM-DD channel.

[1]in the sense that the gap to capacity upper bounds is close to zero.

II. The Intensity-Modulation Direct-Detection Channel

We consider an IM-DD channel whose input $X > 0$ is a random variable representing the intensity of the optical signal. Since intensity is constrained due to practical and safety restrictions by average and peak constraints in general [17], the input random variable has to satisfy $X \leq \mathcal{A}$ and $\mathbb{E}[X] \leq \mathcal{E}$.

To send a message $w \in \{1, \cdots, M\}$ to the destination, the source encodes it into a codeword $\mathbf{X}(w) = (X_1(w), \cdots, X_n(w))$ of length n symbols, and sends this codeword over the channel. Here, the symbols $X_i(w)$ are realizations of the random variable X. An intensity detector is used at the destination to detect $\mathbf{X}(w)$. The received signal after the detector is

$$\mathbf{Y} = \mathbf{X} + \mathbf{Z}$$

where $\mathbf{Z}$ is a sequence of n independent and identically distributed $g_{0,\sigma}(z)$ noise instances, independent of X. Throughout the paper, we denote the peak signal-to-noise ratio (PSNR) $\frac{\mathcal{A}}{\sigma}$ by γ, and the average signal-to-noise ratio (ASNR) $\frac{\mathcal{E}}{\sigma}$ by $\bar{\gamma}$. In general, we say that the IM-DD has high SNR if $\bar{\gamma} \gg 1$, which for a given APR $\frac{\mathcal{E}}{\mathcal{A}}$, implies that $\gamma \gg 1$.

The destination uses a decoder to recover $\hat{w} \in \{1, \cdots, M\}$ from the received signal $\mathbf{Y}$. An error occurs if $\hat{w} \neq w$, and has a probability P_e. The goal of the paper is to bound the capacity $\mathcal{C}$ of the given IM-DD channel (in units of nats per channel use), defined as the maximum achievable transmission rate. The transmission rate is defined as $R = \frac{\log(M)}{n}$, where R is said to be achievable if the error probability P_e can be made arbitrarily small $P_e \to 0$ by letting $n \to \infty$.

The capacity of the channel can be expressed as

$$\mathcal{C} = \max_{f(x)\in\mathcal{F}} I(X;Y)$$

[25], where $f(x)$ is a distribution of X and $\mathcal{F}$ is the set of distributions of $X \in [0, \mathcal{A}]$ satisfying $\mathbb{E}[X] \leq \mathcal{E}$. Although it is known that the capacity achieving distribution of such a channel is discrete [16], this distribution is yet unknown explicitly. The main goal of this work is to study the capacity of the channel, and to provide simple approximations of this capacity that can be useful in practice.

III. Main Results

We first present a simple result on the optimal $\mathbb{E}[X]$ as given in the following lemma.

Lemma 1: The solution of $\mathcal{C} = \max_{f(x)\in\mathcal{F}} I(X;Y)$ satisfies $\mathbb{E}[X] = \min\left\{\mathcal{E}, \frac{\mathcal{A}}{2}\right\}$.

Proof: The proof is given in Appendix A. ∎

Note that this generalizes the result in [11, Proposition 9] stating that the capacity of this channel admits a maximum at $\mathbb{E}[X] = \frac{\mathcal{A}}{2}$.

The next results concerns the IM-DD channel with a peak constraint only.

This article has been accepted for publication in a future issue of this journal, but has not been fully edited. Content may change prior to final publication. Citation information: DOI 10.1109/TCOMM.2016.2524569, IEEE Transactions on Communications

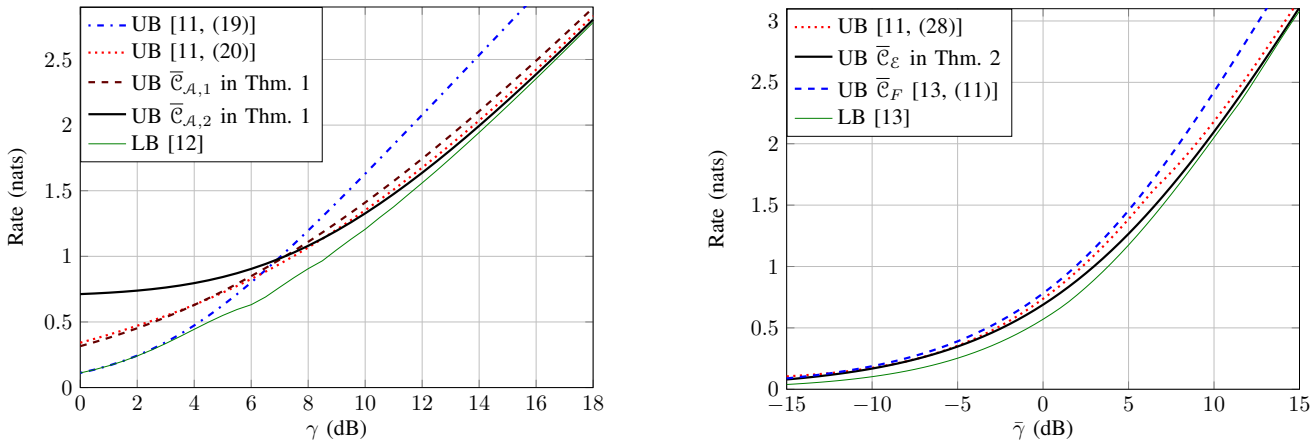

(a) Peak only.

(b) Average only.

Fig. 1: A comparison between different capacity upper bounds (UB) and lower bounds (LB) for an IM-DD channel with either a peak constraint of an average constraint.

Theorem 1: The capacity $\mathcal{C}_{\mathcal{A}}$ of a channel with a peak constraint only satisfies $\mathcal{C}_{\mathcal{A}} \leq \overline{\mathcal{C}}_{\mathcal{A},i}$, $i \in \{1,2\}$, where $\overline{\mathcal{C}}_{\mathcal{A},i} = \sup_{\alpha\in[0,1]} B_i(\alpha)$ and

$$B_1(\alpha) = \alpha \log\left(\frac{\gamma}{\sqrt{2\pi e}}\right) - \log\left(\alpha^{\alpha}(1-\alpha)^{\frac{3(1-\alpha)}{2}}\right)$$
$$B_2(\alpha) = \alpha \log\left(\frac{\gamma}{\sqrt{2\pi e}}\right) - \log\left(\alpha^{\frac{\alpha}{2}}(1-\alpha)^{1-\alpha}2^{\alpha-1}\right).$$

Proof: The proof is given in Section IV. ■

Those bounds are derived using sphere-packing arguments, by bounding the number of disjoint spheres [13], [26] that can be packed centered within a cube of side-length $\mathcal{A}$. This problem can be approached by using the Steiner-Minkowski formula as [13] leading to $\overline{\mathcal{C}}_{\mathcal{A},1}$. We propose a new approach based on a recursive argument which leads to $\overline{\mathcal{C}}_{\mathcal{A},2}$. The main idea of the recursive approach is bounding the number of spheres (and portions thereof) inside an n-dimensional cube, then inside its $(n-i)$-dimensional faces which are $(n-i)$-dimensional cubes, for $i = 1, \cdots, n$.

Fig. 1a shows several capacity bounds as a function of the PSNR γ for a channel with a peak constraint *only*. Note that the upper bound $\overline{\mathcal{C}}_{\mathcal{A},2}$ is the tightest at moderate/high PSNR ($\gamma > 8$ dB), and that it converges faster to the high PSNR capacity of the channel. For comparison, the best known lower bound from [12] is shown. This lower bound is achievable by using a discrete uniform input distribution with equally spaced mass points, i.e., by solving $\max_{K\geq 1} I(X;Y)$ where X follows the distribution $f(x) = \sum_{k=0}^{K} \frac{1}{K+1}\delta(x-k\ell)$, $\ell = \mathcal{A}/K$, and $\delta(\cdot)$ is the Dirac delta function. The bounds [11, (19)] and $\overline{\mathcal{C}}_{\mathcal{A},2}$ provide a tight capacity characterization at low and high PSNR, respectively.

Under an average constraint only, we have the following bound.

Theorem 2: The capacity $\mathcal{C}_{\mathcal{E}}$ of a channel with an average constraint only satisfies $\mathcal{C}_{\mathcal{E}} \leq \overline{\mathcal{C}}_{\mathcal{E}}$ where $\overline{\mathcal{C}}_{\mathcal{E}} = \sup_{\alpha\in[0,1]} B_3(\alpha)$, and

$$B_3(\alpha) = \alpha \log\left(\frac{\sqrt{e}\bar{\gamma}}{\sqrt{2\pi}}\right) - \log\left((1-\alpha)^{1-\alpha}\alpha^{\frac{3\alpha}{2}}\right). \quad (1)$$

Proof: The proof is given in Section V. ■

This bound is derived using sphere-packing in a simplex with our recursive approach. The Steiner-Minkowski formula was used in [13] to obtain the bound $\mathcal{C}_{\mathcal{E}} \leq \overline{\mathcal{C}}_{F} = \sup_{\alpha\in[0,1]} B_4(\alpha)$ where

$$B_4(\alpha) = B_3(\alpha) + \frac{\alpha}{2}\log\left(\frac{e}{2}\right) - \frac{1}{2}\log\left(\frac{(1-\frac{\alpha}{2})^{2-\alpha}}{(1-\alpha)^{1-\alpha}}\right).$$

By direct comparison, it can be shown that $B_3(\alpha) \leq B_4(\alpha)$ for all $\alpha \in [0,1]$ with equality if $\alpha = 0$. Our upper bound is tighter because it exploits the geometry of the ball as we shall see in Section V. The bound $\overline{\mathcal{C}}_{\mathcal{E}}$ coincides at high ASNR with the capacity of the channel with an average constraint *only* given in [11, Proposition 8], but has a simpler expression. Fig. 1b shows several capacity bounds as a function of ASNR $\bar{\gamma}$. Note that our bound $\overline{\mathcal{C}}_{\mathcal{E}}$ is closest to the best known lower bound from [13]. This lower bound is achieved by using a geometric input distribution with equally spaced mass points, i.e., by solving $\max_{\ell>0} I(X;Y)$ where X follows the distribution $f(x) = \sum_{k=0}^{\infty} \frac{\ell}{\ell+\mathcal{E}}\left(\frac{\mathcal{E}}{\ell+\mathcal{E}}\right)^{k}\delta(x-k\ell)$.

Since dropping constraints does not decrease capacity, the capacity under both average and peak constraints is upper bounded by that under one constraint only. This leads to the following corollary.

Corollary 1: The capacity $\mathcal{C}$ of an IM-DD channel with an average constraint $\mathcal{E}$ and a peak constraint $\mathcal{A}$ is upper bounded by $\overline{\mathcal{C}}_{\mathcal{E}}$, $\overline{\mathcal{C}}_{\mathcal{A},1}$, and $\overline{\mathcal{C}}_{\mathcal{A},2}$.

The bounds $\overline{\mathcal{C}}_{\mathcal{A},1}$ and $\overline{\mathcal{C}}_{\mathcal{A},2}$ are tight at high SNR if $\frac{\mathcal{E}}{\mathcal{A}} \geq \frac{1}{2}$ which reproduces the high-SNR result in [11, Corollary 6]. As we shall show, the upper bound $\overline{\mathcal{C}}_{\mathcal{E}}$ is fairly tight at high SNR if $\frac{\mathcal{E}}{\mathcal{A}} < \frac{1}{2}$.

Another capacity upper bound for this case, which is tight at low SNR, was given in [11, (11) & (19)]. This upper bound is given as follows.

This article has been accepted for publication in a future issue of this journal, but has not been fully edited. Content may change prior to final publication. Citation information: DOI 10.1109/TCOMM.2016.2524569, IEEE Transactions on Communications

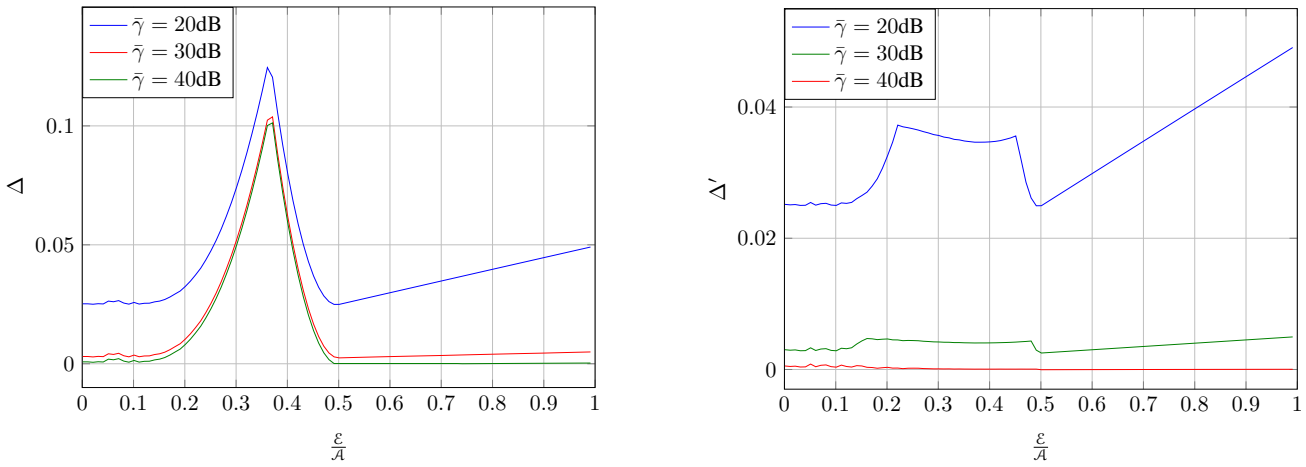

(a) $\Delta = \min\{\overline{\mathcal{C}}_{\mathcal{E}}, \overline{\mathcal{C}}_{\mathcal{A},2}\} - \mathcal{R}'$.

(b) $\Delta' = \min\{\overline{\mathcal{C}}_{\mathcal{E}}, \overline{\mathcal{C}}_{\mathcal{A},2}, \overline{\mathcal{C}}_{L,1}\} - \mathcal{R}'$.

Fig. 2: The gap between the sphere-packing bounds and the truncated-Gaussian lower bound for different ratios $\frac{\mathcal{E}}{\mathcal{A}}$.

Theorem 3 ([11, (11) & (19)]): The capacity $\mathcal{C}$ satisfies $\mathcal{C} \leq \overline{\mathcal{C}}$ where $\overline{\mathcal{C}} = \frac{1}{2}\log\left(1+\frac{\gamma^2}{4}\right)$ if $\frac{\mathcal{E}}{\mathcal{A}} \geq \frac{1}{2}$ and $\overline{\mathcal{C}} = \frac{1}{2}\log\left(1+\bar{\gamma}(\gamma-\bar{\gamma})\right)$ otherwise.

Proof: This bound was derived in [11] using a duality approach. An alternative proof of this theorem is given in Section VI-A. ∎

After deriving the aforementioned upper bounds, we derive a capacity lower bound. This lower bound is given by the achievable rate of a truncated-Gaussian (TG) input distribution satisfying both average and peak constraints, as given in the following theorem.

Theorem 4: The capacity $\mathcal{C}$ satisfies $\mathcal{C} \geq \mathcal{R} \geq \mathcal{R}'$ where the achievable rates $\mathcal{R}$ and $\mathcal{R}'$ are given by $\mathcal{R} = \mathcal{R}' - \Phi_3(\mu,\nu)$ and $\mathcal{R}' = \mathcal{C}_0(\nu) - \Phi_1(\mu,\nu) - \Phi_2(\mu,\nu)$, and where $\mathcal{C}_0(\nu) = \frac{1}{2}\log\left(1+\frac{\nu^2}{\sigma^2}\right)$, $\Phi_1(\mu,\nu) = \log(\eta)$,

$$\Phi_2(\mu,\nu) = \left((\mathcal{A}-\mu)g_{\mu,\nu}(\mathcal{A}) + \mu g_{\mu,\nu}(0)\right)\frac{\eta\nu^2}{2(\nu^2+\sigma^2)},$$
$$\Phi_3(\mu,\nu) = \mathbb{E}_{X,Y}\left[\log(G_{\mu',\nu'}(\mathcal{A}) - G_{\mu',\nu'}(0))\right],$$

for some parameters μ and ν satisfying $\nu^2\eta(g_{\mu,\nu}(0) - g_{\mu,\nu}(\mathcal{A})) + \mu \leq \min\{\mathcal{E}, \frac{\mathcal{A}}{2}\}$, with $\eta = (G_{\mu,\nu}(\mathcal{A}) - G_{\mu,\nu}(0))^{-1}$, $\mu' = \frac{\mu\sigma^2+y\nu^2}{\nu^2+\sigma^2}$, $\nu' = \frac{\nu\sigma}{\sqrt{\nu^2+\sigma^2}}$, and the expectation in $\Phi_3(\mu,\nu)$ is taken with respect to the distribution $f(x,y) = \eta g_{\mu,\nu}(x) g_{x,\sigma}(y)$ over $x \in [0,\mathcal{A}]$ and $y \in \mathbb{R}$.

Proof: See Sec. VI-B. ∎

Although $\mathcal{R}$ is higher than the achievable rates given in [11, (10) & (18)], it has a sophisticated expression. However, $\mathcal{R}'$ is simpler to compute, and is also simpler than $\mathcal{R}_F$ in [12]. At high SNR, specific choices of μ and ν lead to $\mathcal{R}'$ being close to the sphere-packing bounds as we shall see in Sec. VI-B. By numerically optimizing with respect to μ and ν, we observe that $\mathcal{R}'$ is within a gap of ≈ 0 and < 0.1 nats per channel use at high SNR of the sphere-packing bounds $\overline{\mathcal{C}}_{\mathcal{A},2}$ and $\overline{\mathcal{C}}_{\mathcal{E}}$ for $\frac{\mathcal{E}}{\mathcal{A}} \geq \frac{1}{2}$ and $\frac{\mathcal{E}}{\mathcal{A}} < \frac{1}{2}$, respectively (Fig. 2a). This negligible gap at high SNR leads to the following approximation.

Proposition 1: The high-SNR capacity of a channel with both average and peak constraints can be well-approximated by $\mathcal{C}_{\text{High SNR}} \approx \min\left\{\frac{1}{2}\log\left(\frac{e\bar{\gamma}^2}{2\pi}\right), \frac{1}{2}\log\left(\frac{\gamma^2}{2\pi e}\right)\right\}$.

These expressions are limits of $\overline{\mathcal{C}}_{\mathcal{E}}$ and $\overline{\mathcal{C}}_{\mathcal{A},2}$ as $\gamma \to \infty$. The approximation gap is at most 0.1 nats.

Remark 1: It can be shown numerically that $\mathcal{R}'$ (and consequently $\mathcal{R}$) is *nearly* capacity achieving at high SNR. This statement is based on the negligible gap, at high SNR, between $\mathcal{R}'$ and the upper bound given by $\min\{\overline{\mathcal{C}}_{\mathcal{E}}, \overline{\mathcal{C}}_{L,1}, \overline{\mathcal{C}}_{\mathcal{A},2}\}$ with $\overline{\mathcal{C}}_{L,1}$ being the bound given in [11, (12)] (see Fig. 2b).

Remark 2: The high-SNR capacity of a channel with both average and peak constraints is within ≈ 0 and 0.1 nats at most of the sphere-packing bound $\overline{\mathcal{C}}_{\mathcal{E}}$ for $\frac{\mathcal{E}}{\mathcal{A}} \leq 0.15$ and $0.15 < \frac{\mathcal{E}}{\mathcal{A}} \leq \frac{1}{e}$, respectively (see Fig. 2). This bounds is in turn tight at high SNR for a channel with an average constraint only. Therefore, for a channel with an average constraint only, imposing a peak constraint $\mathcal{A} \geq e\mathcal{E}$ or $\mathcal{A} \geq \frac{20}{3}\mathcal{E}$ leads to a high SNR capacity loss of at most 0.1 nats or ≈ 0, respectively.

The bounds are plotted in Fig. 3. In general, the sphere-packing bounds $\overline{\mathcal{C}}_{\mathcal{E}}$ and $\overline{\mathcal{C}}_{\mathcal{A},2}$ are fairly tight at moderate/high SNR. The bound $\overline{\mathcal{C}}_{\mathcal{E}}$ is tighter than $\overline{\mathcal{C}}_{\mathcal{A},2}$ when the $\frac{\mathcal{E}}{\mathcal{A}}$ is small (thus, we do not plot $\overline{\mathcal{C}}_{\mathcal{A},2}$ in Fig. 3a and 3b). The transition point where $\overline{\mathcal{C}}_{\mathcal{A},2}$ becomes tighter than $\overline{\mathcal{C}}_{\mathcal{E}}$ occurs around $\frac{\mathcal{E}}{\mathcal{A}} = \frac{1}{e}$. At this point, the bound given in [11, (12)] which we denote $\overline{\mathcal{C}}_{L,1}$, becomes slightly tighter than $\overline{\mathcal{C}}_{\mathcal{A},2}$. The reason is that under both constraints, the feasible region of the codeword $\mathbf{X}$ is the intersection of a simplex and a cube. At moderate $\frac{\mathcal{E}}{\mathcal{A}}$, treating this intersection as either a simplex or a cube enlarges the upper bound. In summary, the bounds $\overline{\mathcal{C}}_{\mathcal{E}}$, $\overline{\mathcal{C}}$, $\overline{\mathcal{C}}_{L,1}$, and $\mathcal{R}_F$ provide the tightest capacity bounding for all SNR for $\frac{\mathcal{E}}{\mathcal{A}} < \frac{1}{e}$. On the other hand, the bounds $\overline{\mathcal{C}}_{\mathcal{A},2}$, $\overline{\mathcal{C}}$, $\overline{\mathcal{C}}_{L,2}$ [11, (20)], and $\mathcal{R}_F$ provide the tightest capacity bounding for all SNR for $\frac{\mathcal{E}}{\mathcal{A}} > \frac{1}{e}$.

Simple capacity expressions are of theoretical importance since they can be used to study fading channels [24], [27]. From this point of view, it is interesting to find simple fitting functions which capture the best known achievable rate $\mathcal{R}_F$ given in [12]. It turns out that a globally close fit for $\mathcal{R}_F$ can

This article has been accepted for publication in a future issue of this journal, but has not been fully edited. Content may change prior to final publication. Citation information: DOI 10.1109/TCOMM.2016.2524569, IEEE Transactions on Communications

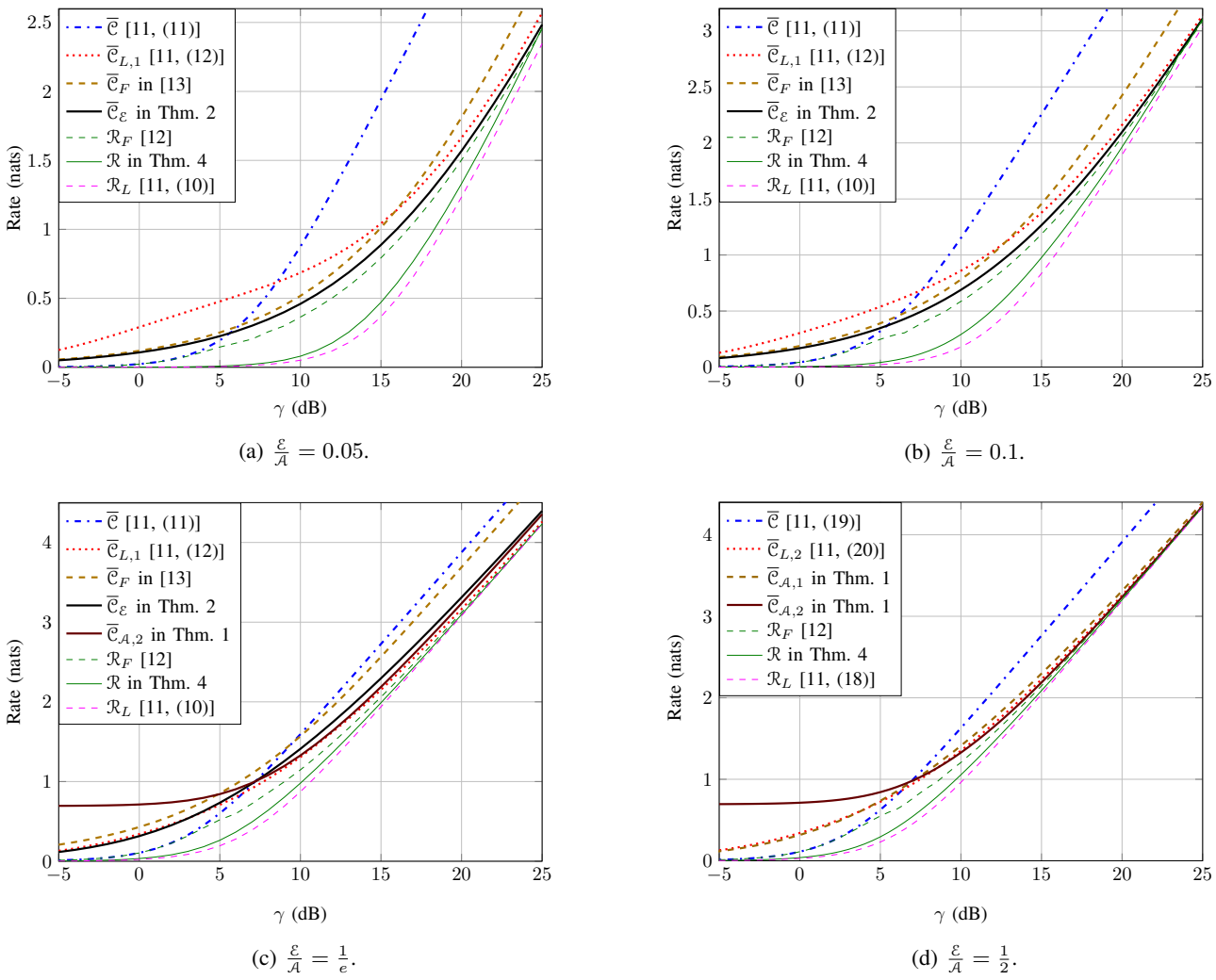

(a) $\frac{\mathcal{E}}{\mathcal{A}} = 0.05$. (b) $\frac{\mathcal{E}}{\mathcal{A}} = 0.1$.

(c) $\frac{\mathcal{E}}{\mathcal{A}} = \frac{1}{e}$. (d) $\frac{\mathcal{E}}{\mathcal{A}} = \frac{1}{2}$.

Fig. 3: The capacity upper bounds and lower bounds plotted versus the signal-to-noise ratio γ for several ratios $\frac{\mathcal{E}}{\mathcal{A}}$. Note that $\frac{\mathcal{E}}{\mathcal{A}} = \frac{1}{2}$ represents all scenarios with $\frac{\mathcal{E}}{\mathcal{A}} \geq \frac{1}{2}$ (including the case with only a peak constraint) since they have the same capacity [11].

be obtained by using the function

$$\Psi(\gamma) = \frac{1}{2}\log\left(1+\gamma^2\left(c_1+(c_2-c_1)\frac{\Theta_1(\gamma)}{\Theta_2(\gamma)}\right)\right),$$

where $c_1 = \min\left\{\frac{e\bar{\gamma}^2}{2\pi\gamma^2}, \frac{1}{2\pi e}\right\}$, $c_2 = \min\left\{\frac{\bar{\gamma}}{\gamma}\left(1-\frac{\bar{\gamma}}{\gamma}\right), \frac{1}{4}\right\}$, and where $\Theta_1(\gamma)$ and $\Theta_2(\gamma)$ are polynomials of degrees m_1 and $m_2 > m_1$ in γ, respectively. Choosing $(m_1, m_2) = (0, 1)$ gives a good fit, with a slight improvement by choosing $(m_1, m_2) = (1, 2)$. The coefficients of the polynomials $\Theta_1(\gamma)$ and $\Theta_2(\gamma)$ can be obtained by solving a system of linear equations as we shall see in Section VII. A rather simpler local fit is given by the function

$$\widehat{\Psi}(\gamma) = \frac{d_1}{2}\log(1+d_2\gamma^2),$$

for γ in a given desired range of operation, where d_1 and d_2 are to be chosen based on the desired SNR range. The parameters d_1 and d_2 can be chosen for a range $\gamma \in [\gamma_1, \gamma_2]$ dB using a simple formula, and the achievable rates of $\mathcal{R}_F$ at three PSNR values, γ_1, γ_2, and $\gamma_0 \in [\gamma_1, \gamma_2]$. This function provides a very good local fit for the SNR range of interest, and can be used to study channels with weak turbulence where the SNR does not vary widely.

The next sections prove the main results presented in this section.

IV. The IM-DD Channel with a Peak Constraint

Upper bounds and lower bounds for this case have been derived in [11]. Here, we present upper bounds on the capacity based on sphere-packing arguments. We consider two approaches: one that uses the Steiner-Minkowski formula, and one that uses a recursive approach. Then, we compare the two approaches and comment on their differences.

Since a codeword $\mathbf{X} = (X_1, X_2, \cdots, X_n)$ satisfies the constraint $0 \leq X_i \leq \mathcal{A}$ for $i = 1, \cdots, n$, then this codeword is confined to an n-dimensional cube with edge-length $\mathcal{A}$, which we denote $\mathcal{W}_{\mathcal{A}}^n$.

On the other hand, the noise Z satisfies $\mathbb{E}[Z^2] = \sigma^2$. Thus, for large n, the noise $\mathbf{Z}$ is confined "almost certainly to some

This article has been accepted for publication in a future issue of this journal, but has not been fully edited. Content may change prior to final publication. Citation information: DOI 10.1109/TCOMM.2016.2524569, IEEE Transactions on Communications

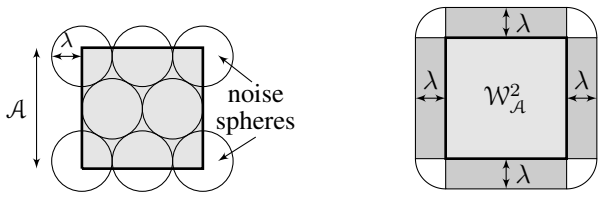

(a) A 2-dimensional illustration of sphere-packing in a cube.

(b) The λ-neighborhood of the square is the sum of a square, a disk, and four rectangles.

Fig. 4: Packing spheres of radius λ so that their center lie inside a cube of side-length $\mathcal{A}$. The convex envelope at a distance λ of the cube is the λ-neighborhood of the cube.

point near the surface" [26] of an n-dimensional ball of radius

$$\lambda \triangleq \sqrt{n\sigma^2}$$

by the sphere hardening effect [28, Chapter 5]. We denote this ball by $\mathcal{B}_\lambda^n$.

Thus, the noise-perturbed signal $\mathbf{Y} = \mathbf{X} + \mathbf{Z}$ lies almost surely near the surface of a ball $\mathcal{B}_\lambda^n$ about $\mathbf{X}$. This is denoted "decoding sphere" in [25]. An upper bound for the IM-DD channel capacity can be obtained by computing the maximum number M_n of disjoint decoding spheres that can be packed centered in $\mathcal{W}_{\mathcal{A}}^n$ (Fig. 4a), as $n \to \infty$.[2]

A. Steiner-Minkowski Formula

An upper bound on M_n can be found using an idea similar to the sphere-packing argument in [25]. The main difference is that in our case we have a cube instead of a sphere.

The noise balls extend $\mathcal{W}_{\mathcal{A}}^n$ by a distance of λ in all directions. This extension is the so-called λ-neighborhood of $\mathcal{W}_{\mathcal{A}}^n$,[3] which we denote by $\mathcal{W}_{\mathcal{A}}^n(\lambda)$. By dividing the volume of $\mathcal{W}_{\mathcal{A}}^n(\lambda)$ by the volume of $\mathcal{B}_\lambda^n$, we get an upper bound on M_n. This leads to a upper bound on $\mathcal{C}_{\mathcal{A}}$, the capacity of a channel with a peak constraint only, as follows:

$$\mathcal{C}_{\mathcal{A}} \leq \lim_{n\to\infty} \frac{1}{n} \log\left(\frac{V(\mathcal{W}_{\mathcal{A}}^n(\lambda))}{V(\mathcal{B}_\lambda^n)}\right).$$

Finding $V(\mathcal{W}_{\mathcal{A}}^n(\lambda))$ is not as straightforward as the case of a sphere. However, according to the Steiner-Minkowski theorem for polytopes [18, Proposition 12.3.6], this volume can be written as a polynomial of degree n in λ. This theorem is stated as follows.

Theorem 5 (Steiner-Minkowski [18]): To every n-dimensional convex set $\mathcal{T}$, we can associate scalars $L_i(\mathcal{T})$, $i = 0, 1, \cdots, n$, such that the volume of the λ-neighborhood $\mathcal{T}'(\lambda)$ of $\mathcal{T}$, $\lambda > 0$, is given by $V(\mathcal{T}(\lambda)) = \sum_{i=0}^n L_i(\mathcal{T})\lambda^i$, where $L_i(\mathcal{T})$ are continuous functions.

Thus, for evaluating $V(\mathcal{W}_{\mathcal{A}}^n(\lambda))$, it remains to determine the coefficients of the Steiner-Minkowski formula. These coefficients were given in [19] for any convex body as follows.

Theorem 6 ([19]): For any convex body $\mathcal{T}$ of n dimensions, the coefficients of the Steiner-Minkowski formula can be written as $L_i(\mathcal{T}) = \sum_{\mathcal{T}^{n-i}\in\partial\mathcal{T}} V(\mathcal{T}^{n-i})V(\mathcal{B}_1^i)\theta_{\mathcal{T}^{n-i},\mathcal{T}}$, where $\mathcal{T}^{n-i}$ is a generic $n-i$ dimensional face of $\partial\mathcal{T}$ the boundary of $\mathcal{T}$, and $\theta_{\mathcal{T}^{n-i},\mathcal{T}}$ is the normalized dihedral external angle of $\mathcal{T}^{n-i}$ in $\mathcal{T}$.

Example: An example illustrating this theorem is shown in Fig. 4b. This figure shows $\mathcal{W}_{\mathcal{A}}^2(\lambda)$, the λ-neighborhood of $\mathcal{W}_{\mathcal{A}}^2$. Note that the extension of $\mathcal{W}_{\mathcal{A}}^2$ by λ extends each vertex to a quarter of a 2-dimensional disk of radius λ, and each edge to a half of a 2-dimensional cylinder (rectangle) of length $\mathcal{A}$ and radius λ. Thus we can write

$$\begin{aligned} V(\mathcal{W}_{\mathcal{A}}^2(\lambda)) &= \mathcal{A}^2 + 4(2^{-1})\mathcal{A}^1(2\lambda) + 4(2^{-2})\mathcal{A}^0(\pi\lambda^2) \\ &= \sum_{i=0}^n 2^i \binom{n}{n-i} 2^{-i}\mathcal{A}^{n-i}V(\mathcal{B}_\lambda^i), \end{aligned}$$

with $n = 2$. In this expression, $2^i\binom{n}{n-i}$ is the number of $n-i$ dimensional faces of $\mathcal{W}_{\mathcal{A}}^n$ [18], 2^{-i} is the normalized dihedral external angle of the $n-i$ dimensional face in $\mathcal{W}_{\mathcal{A}}^n$ (see definition of this angle in [19]), and $\mathcal{A}^i V(\mathcal{B}_\lambda^i)$ is the volume of the cylinder formed by the orthogonal product of the $n-i$ dimensional face and $\mathcal{B}_\lambda^i$. Note that the $n-i$ dimensional faces of $\mathcal{W}_{\mathcal{A}}^n$ are $\mathcal{W}_{\mathcal{A}}^{n-i}$ [18].

Applying Theorem 6 for the cube $\mathcal{W}_{\mathcal{A}}^n$ leads to $L_i(\mathcal{W}_{\mathcal{A}}^n)\lambda^i = \binom{n}{n-i}\mathcal{A}^{n-i}V(\mathcal{B}_\lambda^i)$. Now, we replace $V(\mathcal{B}_\lambda^i)$ by $\frac{(\sqrt{\pi}\lambda)^i}{\Gamma\left(1+\frac{i}{2}\right)}$ ($\Gamma(\cdot)$ is the Gamma function) and λ by $\sqrt{n\sigma^2}$, we substitute $L_i(\mathcal{W}_{\mathcal{A}}^n)$ in the expression of $V(\mathcal{W}_{\mathcal{A}}^n(\lambda))$ according to Theorem 5, and divide by $V(\mathcal{B}_\lambda^n)$ to obtain

$$M_n \leq \frac{V(\mathcal{W}_{\mathcal{A}}^n(\lambda))}{V(\mathcal{B}_\lambda^n)} = \sum_{i=0}^n N_i, \tag{2}$$

where $N_i = \binom{n}{n-i}\left(\frac{\mathcal{A}}{\sqrt{\pi n\sigma^2}}\right)^{n-i}\frac{\Gamma\left(1+\frac{n}{2}\right)}{\Gamma\left(1+\frac{i}{2}\right)}$.

Thus, we have the upper bound $\mathcal{C}_{\mathcal{A}} \leq \overline{\mathcal{C}}_{\mathcal{A},1} = \lim_{n\to\infty}\frac{1}{n}\log\left(\sum_{i=0}^n N_i\right)$ from (2). The remaining steps are similar to [13] (given in Appendix B for completeness), and lead to

$$\lim_{n\to\infty}\frac{1}{n}\log\left(\sum_{i=0}^n N_i\right) \leq \sup_{\alpha\in[0,1]} B_1(\alpha), \tag{3}$$

where $B_1(\alpha)$ is as given in Theorem 1.

Note that apart from defining the λ-neighborhood of the cube $\mathcal{W}_{\mathcal{A}}^n$, the rest of the derivation of the bound $\overline{\mathcal{C}}_{\mathcal{A},1}$ is independent of the geometry of the ball since it is based on $\frac{V(\mathcal{W}_{\mathcal{A}}^n(\lambda))}{V(\mathcal{B}_\lambda^n)}$, where only the volume of the ball matters. In fact, the upper bound on M_n in (2) can be interpreted as the number of containers of liquid of volume $V(\mathcal{B}_\lambda^n)$ that can be poured inside $V(\mathcal{W}_{\mathcal{A}}^n(\lambda))$. From this point of view, an approach which better exploits the geometry of the ball should have an advantage over this one, at least in some cases. Next, we present a such an approach.

B. A Recursive Approach

Recall that an upper bound on the channel capacity can be obtained by computing the maximum number M_n of disjoint

[2] See [28, Chapter 5] for a detailed justification of this sphere-packing bounding approach. Another geometric justification of this approach is given in [29, Appendix B].

[3] or the Minkowski sum of the cube and the ball

This article has been accepted for publication in a future issue of this journal, but has not been fully edited. Content may change prior to final publication. Citation information: DOI 10.1109/TCOMM.2016.2524569, IEEE Transactions on Communications

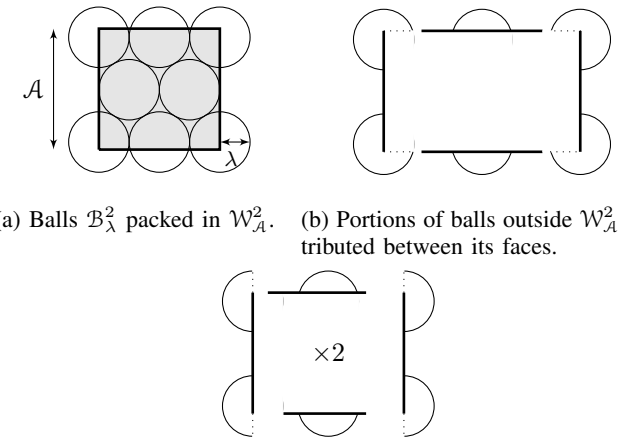

(a) Balls $\mathcal{B}_\lambda^2$ packed in $\mathcal{W}_\mathcal{A}^2$.

(b) Portions of balls outside $\mathcal{W}_\mathcal{A}^2$ distributed between its faces.

(c) Upper bound for the portions in Fig. 5b.

Fig. 5: A 2-dimensional illustration of the recursive approach.

balls $\mathcal{B}_\lambda^n$ that can be packed centered in $\mathcal{W}_\mathcal{A}^n$, as $n \to \infty$ [13], [25], [26]. Consider an arbitrary constellation of such balls. We upper bound the number of balls M_n by upper bounding their total volume[4] and then dividing by $V(\mathcal{B}_\lambda^n)$. The total volume of such balls can be written as

$$v_{\text{tot}} = v_{\text{in}}(\mathcal{W}_\mathcal{A}^n) + v_{\text{out}}(\mathcal{W}_\mathcal{A}^n), \tag{4}$$

where $v_{\text{in}}(\mathcal{W}_\mathcal{A}^n)$ is the total volume of balls and portions of balls inside $\mathcal{W}_\mathcal{A}^n$, and $v_{\text{out}}(\mathcal{W}_\mathcal{A}^n)$ is the total volume of portions of balls outside $\mathcal{W}_\mathcal{A}^n$. Clearly, $v_{\text{in}}(\mathcal{W}_\mathcal{A}^n) \leq V(\mathcal{W}_\mathcal{A}^n)$ (shaded area in the 2-dimensional illustration in Fig. 5a). Now we upper bound $v_{\text{out}}(\mathcal{W}_\mathcal{A}^n)$ (unshaded areas in Fig. 5a).

Consider one $(n-1)$-dimensional face $\mathcal{W}_\mathcal{A}^{n-1}$ of $\mathcal{W}_\mathcal{A}^n$. Our goal is to transform the problem of bounding $v_{\text{out}}(\mathcal{W}_\mathcal{A}^n)$ to a problem of packing $(n-1)$-balls in $\mathcal{W}_\mathcal{A}^{n-1}$. To this end, we distribute the portions of balls outside $\mathcal{W}_\mathcal{A}^n$ between the faces, by associating each portion to the face with which it has the largest intersection (see Fig. 5b). Next, we upper bound the total volumes of these portions by twice the total volumes of the spherical-caps[5] on the outer side of the face (see Fig. 5c), where we multiply by 2 to account for the portions overflowing to the other side of this face. Thus,

$$v_{\text{out}}(\mathcal{W}_\mathcal{A}^n) \leq 2 \sum_{\mathcal{W}_\mathcal{A}^{n-1} \subset \partial \mathcal{W}_\mathcal{A}^n} V(\text{spherical-caps on } \mathcal{W}_\mathcal{A}^{n-1}), \tag{5}$$

where $\partial \mathcal{W}_\mathcal{A}^n$ is the boundary of $\mathcal{W}_\mathcal{A}^n$. Hence,

$$v_{\text{tot}} \leq V(\mathcal{W}_\mathcal{A}^n) + 2 \sum_{\mathcal{W}_\mathcal{A}^{n-1} \subset \partial \mathcal{W}_\mathcal{A}^n} V(\text{spherical-caps on } \mathcal{W}_\mathcal{A}^{n-1}). \tag{6}$$

Next, we upper bound $V(\text{spherical-caps on } \mathcal{W}_\mathcal{A}^{n-1})$. Denote the volume of an n-dimensional spherical-cap of height h and radius λ (see Fig. 6) by $V(\mathcal{P}_{\lambda,h}^n)$. We transform each spherical-cap to an equivalent cylinder which has the same base as the spherical-cap, but different height h', so that both have the same volume. The height h' of this cylinder is $h' = \frac{V(\mathcal{P}_{\lambda,h}^n)}{V(\mathcal{B}_{\lambda'}^{n-1})}$, where $\lambda' = \sqrt{2h\lambda - h^2}$, since the base of the spherical-cap is $\mathcal{B}_{\lambda'}^{n-1}$. In Appendix C, we show that $h' \leq \hat{h}_n$ where $\hat{h}_n$ is the height of the equivalent cylinder corresponding to a spherical cap $\mathcal{P}_{\lambda,\lambda}^n$. Thus

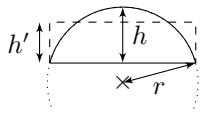

Fig. 6: A spherical-cap in 2-dimensions of radius r and height h, and the corresponding equivalent cylinder (rectangle in the 2-dimensional case) of height h'.

$$h' \leq \hat{h}_n = \frac{V(\mathcal{B}_\lambda^n)}{2V(\mathcal{B}_\lambda^{n-1})}. \tag{7}$$

Therefore, we can write $V(\mathcal{P}_{\lambda,h}^n) \leq \hat{h}_n V(\mathcal{B}_{\lambda'}^{n-1})$.

Now we get back to bounding $V(\text{spherical-caps on } \mathcal{W}_\mathcal{A}^{n-1})$. Denote the heights of spherical-caps on $\mathcal{W}_\mathcal{A}^{n-1}$ by $h_1, \cdots, h_a$ where $a \in \mathbb{N}$ is the number of such caps. Then, we can write

$$V(\text{spherical-caps on } \mathcal{W}_\mathcal{A}^{n-1}) = \sum_{i=1}^{a} V(\mathcal{P}_{\lambda,h_i}^n) \tag{8}$$

$$\leq \hat{h}_n \sum_{i=1}^{a} V(\mathcal{B}_{\lambda_i'}^{n-1}), \tag{9}$$

where $\lambda_i' = \sqrt{2h_i\lambda - h_i^2}$. This step upper bounds the a spherical-caps by a cylinders with larger volume and same intersection with $\mathcal{W}_\mathcal{A}^{n-1}$. At this point, we have a constellation of a balls of dimension $n-1$, whose radii are λ_i', $i = 1, \cdots, a$, and which are centered in $\mathcal{W}_\mathcal{A}^{n-1}$. The total volume of those balls can be upper bounded by repeating the same steps above. Thus,

$$V(\text{spherical-caps on } \mathcal{W}_\mathcal{A}^{n-1}) \leq \hat{h}_n \left[V(\mathcal{W}_\mathcal{A}^{n-1}) + v_{\text{out}}(\mathcal{W}_\mathcal{A}^{n-1}) \right]. \tag{10}$$

Here, $v_{\text{out}}(\mathcal{W}_\mathcal{A}^{n-1})$ is the total volume of the portions of the a $(n-1)$-dimensional balls outside $\mathcal{W}_\mathcal{A}^{n-1}$. We plug this in (6) to obtain

$$\begin{aligned} v_{\text{tot}} &\leq V(\mathcal{W}_\mathcal{A}^n) + 2\hat{h}_n \sum_{\mathcal{W}_\mathcal{A}^{n-1} \subset \partial \mathcal{W}_\mathcal{A}^n} \left[V(\mathcal{W}_\mathcal{A}^{n-1}) + v_{\text{out}}(\mathcal{W}_\mathcal{A}^{n-1}) \right] \\ &= \sum_{i=0}^{1} 2^i K_{n-i} V(\mathcal{W}_\mathcal{A}^{n-i}) \prod_{j=0}^{i} \hat{h}_{n+1-j} \\ &\quad + 2\hat{h}_n \sum_{\mathcal{W}_\mathcal{A}^{n-1} \subset \partial \mathcal{W}_\mathcal{A}^n} v_{\text{out}}(\mathcal{W}_\mathcal{A}^{n-1}), \end{aligned}$$

where K_{n-1} is the number of $(n-1)$-faces in $\mathcal{W}_\mathcal{A}^n$, and where we formally define $\hat{h}_{n+1} = 1$.

Remark 3: While the Steiner-Minkowski approach calculates the volume of the parallel extension of $\mathcal{W}_\mathcal{A}^{n-1}$ of thickness λ, here we have thickness $2\hat{h}_n$ instead, which is smaller than λ for large n.

[4] We refer to the volume of the union of some objects as their "total volume."

[5] A spherical-cap is defined as the portion of an n-sphere cut by an $(n-1)$-plane.

This article has been accepted for publication in a future issue of this journal, but has not been fully edited. Content may change prior to final publication. Citation information: DOI 10.1109/TCOMM.2016.2524569, IEEE Transactions on Communications

Similar to (5), we can show that

$$\sum_{\mathcal{W}_{\mathcal{A}}^{n-1}\subset\partial\mathcal{W}_{\mathcal{A}}^{n}} v_{\text{out}}(\mathcal{W}_{\mathcal{A}}^{n-1}) \leq 2\sum_{\mathcal{W}_{\mathcal{A}}^{n-2}\subset\partial\mathcal{W}_{\mathcal{A}}^{n}} V(\text{spherical-caps on } \mathcal{W}_{\mathcal{A}}^{n-2}). \quad (11)$$

This can be shown by rejoining the $(n-1)$-faces of $\mathcal{W}_{\mathcal{A}}^{n}$, and redistributing the portions of the $(n-1)$-balls over the $(n-2)$-faces of $\mathcal{W}_{\mathcal{A}}^{n}$ in a fashion similar to Fig. 5b. Using (10) again yields[6]

$$v_{\text{tot}} \leq \sum_{i=0}^{2} 2^i K_{n-i} V(\mathcal{W}_{\mathcal{A}}^{n-i}) \prod_{j=0}^{i} \hat{h}_{n+1-j} + 4\hat{h}_n\hat{h}_{n-1}\sum_{\mathcal{W}_{\mathcal{A}}^{n-2}\subset\partial\mathcal{W}_{\mathcal{A}}^{n}} v_{\text{out}}(\mathcal{W}_{\mathcal{A}}^{n-2}) \quad (12)$$

$$= \sum_{i=0}^{\ell} 2^i K_{n-i} V(\mathcal{W}_{\mathcal{A}}^{n-i}) \prod_{j=0}^{i} \hat{h}_{n+1-j} + 2^{\ell}\prod_{j=0}^{\ell}\hat{h}_{n+1-j}\sum_{\mathcal{W}_{\mathcal{A}}^{n-\ell}\subset\partial\mathcal{W}_{\mathcal{A}}^{n}} v_{\text{out}}(\mathcal{W}_{\mathcal{A}}^{n-\ell}) \quad (13)$$

with $\ell = 2$. By proceeding similarly, we can write for $\ell = n-1$

$$v_{\text{tot}} \leq \sum_{i=0}^{n-1} 2^i K_{n-i} V(\mathcal{W}_{\mathcal{A}}^{n-i}) \prod_{j=0}^{i} \hat{h}_{n+1-j} + 2^{n-1}\prod_{j=0}^{n-1}\hat{h}_{n+1-j}\sum_{\mathcal{W}_{\mathcal{A}}^{1}\subset\partial\mathcal{W}_{\mathcal{A}}^{n}} v_{\text{out}}(\mathcal{W}_{\mathcal{A}}^{1}). \quad (14)$$

Similar to (11), we have

$$\sum_{\mathcal{W}_{\mathcal{A}}^{1}\subset\partial\mathcal{W}_{\mathcal{A}}^{n}} v_{\text{out}}(\mathcal{W}_{\mathcal{A}}^{n-1}) \leq 2\sum_{\mathcal{W}_{\mathcal{A}}^{0}\subset\partial\mathcal{W}_{\mathcal{A}}^{n}} V(\text{spherical-caps on } \mathcal{W}_{\mathcal{A}}^{0}). \quad (15)$$

Since $V(\text{spherical-caps on } \mathcal{W}_{\mathcal{A}}^{0})$ is upper bounded by $\hat{h}_1$, we obtain

$$v_{\text{tot}} \leq \sum_{i=0}^{n} 2^i K_{n-i} V(\mathcal{W}_{\mathcal{A}}^{n-i}) \prod_{j=0}^{i} \hat{h}_{n+1-j}. \quad (16)$$

By noting that $2^i\prod_{j=0}^{i}\hat{h}_{n+1-j} = \frac{V(\mathcal{B}_{\lambda}^{n})}{V(\mathcal{B}_{\lambda}^{n-i})}$, and using $K_{n-i} = 2^i\binom{n}{n-i}$, we obtain

$$v_{\text{tot}} \leq \sum_{i=0}^{n} 2^i \binom{n}{n-i} V(\mathcal{W}_{\mathcal{A}}^{n-i}) \frac{V(\mathcal{B}_{\lambda}^{n})}{V(\mathcal{B}_{\lambda}^{n-i})}. \quad (17)$$

Now, we divide by $V(\mathcal{B}_{\lambda}^{n})$, and to obtain the following upper bound on M_n,

$$M_n \leq \sum_{i=0}^{n} 2^i \binom{n}{n-i} \frac{V(\mathcal{W}_{\mathcal{A}}^{n-i})}{V(\mathcal{B}_{\lambda}^{n-i})}. \quad (18)$$

[6]Note that $\hat{h}_n$ is increasing in λ. Thus, the equivalent height of a spherical-cap with radius $\lambda' < \lambda$ is also less than $\hat{h}_n$.

By replacing $V(\mathcal{W}_{\mathcal{A}}^{n-i})$ by $\mathcal{A}^{n-i}$, $V(\mathcal{B}_{\lambda}^{n-i})$ by $\frac{(\sqrt{\pi}\lambda)^n}{\Gamma\left(1+\frac{n}{2}\right)}$, λ by $\sqrt{n\sigma^2}$, and proceeding similar to [13] (see Appendix B), we obtain the upper bound $\mathcal{C}_{\mathcal{A}} \leq \overline{\mathcal{C}}_{\mathcal{A},2} = \sup_{\alpha\in[0,1]} B_2(\alpha)$, where $B_2(\alpha) = \alpha\log\left(\frac{\gamma}{\sqrt{2\pi e}}\right) - \log\left(\alpha^{\frac{\alpha}{2}}(1-\alpha)^{1-\alpha}2^{\alpha-1}\right)$ as given in Theorem 1.

C. Comparison

Note that both $\overline{\mathcal{C}}_{\mathcal{A},1}$ and $\overline{\mathcal{C}}_{\mathcal{A},2}$ are tight at high PSNR γ, since both converge to the lower bound [11, Theorem 5] given by $\mathcal{C}_{\mathcal{A}} \geq \frac{1}{2}\log\left(1+\frac{\gamma^2}{2\pi e}\right)$. This is also true for a channel with both a peak and an average constraint, with $\mathcal{A} \leq 2\mathcal{E}$. Note also that $\overline{\mathcal{C}}_{\mathcal{A},2}$ becomes tighter than $\overline{\mathcal{C}}_{\mathcal{A},1}$ when the optimum α is close to 1. This is the case at moderate/high PSNR where the first term of $B_1(\alpha)$ and $B_2(\alpha)$ dominates the bound. This behavior can be justified by Remark 3, which is in turn due to exploiting the geometry of the sphere in the recursive approach. At low PSNR, $\overline{\mathcal{C}}_{\mathcal{A},1}$ is tighter than $\overline{\mathcal{C}}_{\mathcal{A},2}$. The reason is that in the recursive approach, we place a ball on each vertex of the cube (see (15)). Thus, the upper bound on M_n is larger than 2^n at any PSNR. At low PSNR, this term dominates, and $\overline{\mathcal{C}}_{\mathcal{A},2}$ converges to $\log(2)$ (not to zero as for $\overline{\mathcal{C}}_{\mathcal{A},1}$). The next section applies the recursive approach to bound the capacity of the channel with only an average constraint, and proves Theorem 2.

V. The IM-DD Channel with an Average Constraint

Now we consider an IM-DD channel with only an average intensity constraint. A capacity upper bound in this case can be derived by considering sphere-packing in a simplex. A sphere-packing upper bound was derived in [13], [14] using the Steiner-Minkowski formula. Next, we derive an upper bound using the recursive approach as in Section IV-B, and show that this bound is tighter than the one given in [13] for all ASNR.

A. A Recursive Approach

For a channel with an average constraint only, we have $\mathcal{A} = \infty$. Thus, according to Lemma 1, the optimal distribution satisfies $\mathbb{E}[X] = \mathcal{E}$. On the other hand, by the law of large numbers, for any $\epsilon > 0$, we have $\lim_{n\to\infty} P\left(\left|\frac{1}{n}\sum_{i=1}^{n} X_i - \mathbb{E}[X]\right| \geq \epsilon\right) = 0$. Thus a codeword $\mathbf{X} = (X_1, X_2, \cdots, X_n)$ satisfies $X_i \geq 0$ and $\sum_{i=1}^{n} X_i = n\mathcal{E}$ almost certainly for large n. This confines the codewords to a regular $(n-1)$-simplex $\mathcal{S}_{\mathcal{E}}^{n-1} = \left\{\mathbf{X} \in \mathbb{R}_+^n \,|\sum_{i=1}^{n} X_i = n\mathcal{E}\right\}$ with side-length $n\mathcal{E}\sqrt{2}$ (Fig. 7a shows an example with $n = 3$). Here, we need to upper bound the number M_n of disjoint balls $\mathcal{B}_{\lambda}^{n}$ that can be packed with their centers within $\mathcal{S}_{\mathcal{E}}^{n-1}$. Note that the intersection of an n-ball with the $(n-1)$-dimensional hyperplane supporting $\mathcal{S}_{\mathcal{E}}^{n-1}$ is $\mathcal{B}_{\lambda}^{n-1}$. Thus, the problem is equivalent to bounding the number of balls $\mathcal{B}_{\lambda}^{n-1}$ that can be packed centered in $\mathcal{S}_{\mathcal{E}}^{n-1}$ (see Fig. 7b). Next, we denote $n-1$ by m.

We apply our recursive approach to derive an upper bound. Similar to Section IV-B, we bound the total volume of balls that can be packed centered in $\mathcal{S}_{\mathcal{E}}^{m}$ and then divide by $V(\mathcal{B}_{\lambda}^{m})$.

This article has been accepted for publication in a future issue of this journal, but has not been fully edited. Content may change prior to final publication. Citation information: DOI 10.1109/TCOMM.2016.2524569, IEEE Transactions on Communications

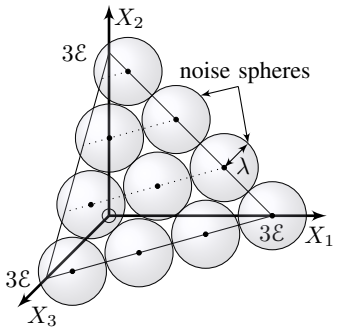

(a) Balls $\mathcal{B}_\lambda^3$ packed centered on the 2-simplex $\mathcal{S}_\mathcal{E}^2$ defined by $\sum_{i=1}^3 X_i = 3\mathcal{E}$.

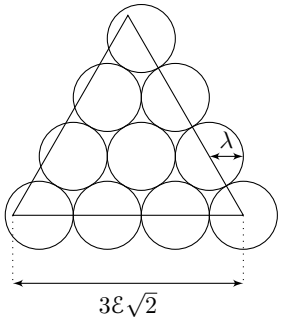

(b) Balls $\mathcal{B}_\lambda^2$ packed on a regular 2-simplex $\mathcal{S}_\mathcal{E}^2$ with side-length $3\mathcal{E}\sqrt{2}$.

Fig. 7

The same steps as (4)–(17) can now be applied to this case. The total volume of balls and portions of balls inside $\mathcal{S}_\mathcal{E}^m$ can be upper bounded by $V(\mathcal{S}_\mathcal{E}^m)$. The portions that extend outwards of $\mathcal{S}_\mathcal{E}^m$ are distributed among the $(m-1)$-dimensional faces of $\mathcal{S}_\mathcal{E}^m$, and bounded by twice the total volume of spherical-caps on the outer side of each face. The spherical-caps are bounded by cylinders, which leads to a problem of packing $(m-1)$-dimensional balls (of different radii) on the $(m-1)$-dimensional faces of $\mathcal{S}_\mathcal{E}^m$. This procedure is repeated for all $(m-i)$-dimensional faces, $i = 0, \cdots, m$. Note that the number of $(m-i)$-dimensional faces, $i = 0, \cdots, m$, in $\mathcal{S}_\mathcal{E}^m$ is $\binom{m+1}{m-i+1}$, and that each such face is in fact an $(m-i)$-simplex [18]. This leads to the following upper bound on the total volume of balls

$$v_{\text{tot}} \leq \sum_{i=0}^{m} \binom{m+1}{m-i+1} V(\mathcal{S}_\mathcal{E}^{m-i}) \frac{V(\mathcal{B}_\lambda^m)}{V(\mathcal{B}_\lambda^{m-i})}. \tag{19}$$

By dividing by $V(\mathcal{B}_\lambda^m)$, we obtain the following upper bound on $M_n = M_{m+1}$

$$M_{m+1} \leq \sum_{i=0}^{m} \binom{m+1}{m-i+1} \frac{V(\mathcal{S}_\mathcal{E}^{m-i})}{V(\mathcal{B}_\lambda^{m-i})}. \tag{20}$$

Using $V(\mathcal{S}_\mathcal{E}^{m-i}) = \frac{(n\mathcal{E})^{m-i}}{(m-i)!}\sqrt{m-i+1}$ [30], $V(\mathcal{B}_\lambda^{m-i}) = \frac{(\sqrt{\pi}\lambda)^{m-i}}{\Gamma\left(1+\frac{m-i}{2}\right)}$, $\lambda = \sqrt{n\sigma^2}$, and proceeding similar to Appendix B, we obtain the upper bound $\mathcal{C}_\mathcal{E} \leq \overline{\mathcal{C}}_\mathcal{E} = \sup_{\alpha\in[0,1]} B_3(\alpha)$, where $B_3(\alpha) = \alpha \log\left(\frac{\sqrt{e}\bar{\gamma}}{\sqrt{2\pi}}\right) - \log\left((1-\alpha)^{1-\alpha}\alpha^{\frac{3\alpha}{2}}\right)$ as given in Theorem 2.

Remark 4: If we use $\mathbb{E}[X] \leq \mathcal{E}$ instead of $\mathbb{E}[X] = \mathcal{E}$, we get the right n-simplex $\hat{\mathcal{S}}_\mathcal{E}^n = \{\mathbf{X} \in \mathbb{R}_+^n | \sum_{i=1}^n X_i \leq n\mathcal{E}\}$. A sphere-packing bound for this case was derived in [13] using the Steiner-Minkowski formula. Our approach can also be applied on this right n-simplex. Alternatively, we can outer bound this right n-simplex by replacing the vertex at the origin with a vertex at $-(d, d, \cdots, d)$ where $d = (\sqrt{n+1}-1)\mathcal{E}$ to obtain a regular n-simplex $\mathcal{S}_\mathcal{E}^n$, and then apply our recursive approach to this simplex. This yields the same bound as (20).

Remark 5: Contrary to the approach by the Steiner-Minkowski formula, our approach avoids using the external normalized dihedral angles which are difficult to compute in a simplex (see [13, (6)]).

B. Comparison

As discussed in Section III, this bound is tighter than the one derived in [13] using the Steiner-Minkowski formula for any ASNR. Again, the main reason is that this recursive approach is more dependent on the geometry of the ball than the approach used in [13]. The bound $\overline{\mathcal{C}}_\mathcal{E}$ characterizes the high ASNR capacity for a channel with *only* an average constraint. Namely, at high ASNR, $B_3(\alpha)$ converges to $\alpha \log\left(\frac{\sqrt{e}\bar{\gamma}}{\sqrt{2\pi}}\right)$, and therefore, $\overline{\mathcal{C}}_\mathcal{E}$ approaches $\frac{1}{2}\log\left(\frac{e\bar{\gamma}^2}{2\pi}\right)$ where it meets the lower bound [11, Theorem 7] given by $\mathcal{C}_\mathcal{E} \geq \frac{1}{2}\log\left(1+\frac{e\bar{\gamma}^2}{2\pi}\right)$.

Recall that using the recursive approach, the bound (20) is dominated by the number of vertexes at low SNR. Since the number of vertexes of the simplex scales linearly with its dimensions, our bound $\overline{\mathcal{C}}_\mathcal{E}$ approaches zero at low ASNR. This is in contrast with $\overline{\mathcal{C}}_{\mathcal{A},2}$ which does not approach zero since the number of vertexes of a cube scales exponentially with its dimensions. Next, we consider an IM-DD channel with both average and peak constraints.

VI. Average and Peak Constraints

Upper bounds on the capacity of the channel with both average and peak constraints were given in [11]. Next, we provide an alternative derivation of one of the bounds in [11].

A. Alternative Derivation of [11, (11) & (19)]

The capacity of the channel is given by $\mathcal{C} = \max_{f(x)\in\mathcal{F}} I(X;Y)$ [25]. The capacity maximizing input distribution is not known. However, we know that if X is unbounded and it satisfies only a variance constraint $\text{Var}(X) \leq P$ ($\text{Var}(X)$ denotes the variance of X), then the maximizing input distribution is $g_{0,\sqrt{P}}(x)$. Assuming that the input of our IM-DD channel satisfies $\text{Var}(X) \leq P$ for some $P > 0$, and ignoring the constraint $X \in [0, \mathcal{A}]$ leads to the upper bound $\mathcal{C} \leq \frac{1}{2}\log\left(1+\frac{P}{\sigma^2}\right)$.

The problem boils down to finding the maximum allowable variance for $f(x) \in \mathcal{F}$. For any distribution $f(x)$ with support

This article has been accepted for publication in a future issue of this journal, but has not been fully edited. Content may change prior to final publication. Citation information: DOI 10.1109/TCOMM.2016.2524569, IEEE Transactions on Communications

$\mathcal{X} \subseteq [0, \mathcal{A}]$ and mean $\mathbb{E}[X] = \mu$, the variance is upper bounded by

$$\begin{aligned} \mathrm{Var}(X) &= \int_{x\in\mathcal{X}} (x-\mu)^2 f(x)dx \qquad (21)\\ &\le \int_{x\in\mathcal{X}} \left[\frac{x}{\mathcal{A}}(\mathcal{A}-\mu)^2 + \left(1-\frac{x}{\mathcal{A}}\right)\mu^2\right] f(x)dx \\ &= \mu(\mathcal{A}-\mu), \qquad (22)\end{aligned}$$

with equality if $f(x) = f_\mu(x)$, the binary distribution with $f_\mu(\mathcal{A}) = \frac{\mu}{\mathcal{A}}$ and $f_\mu(0) = 1 - \frac{\mu}{\mathcal{A}}$. For $f(x) = f_\mu(x)$ with $\mu \le \mathcal{E}$, the variance of X is maximized if $\mu = \frac{\mathcal{A}}{2}$ when $\frac{\mathcal{E}}{\mathcal{A}} \ge \frac{1}{2}$ and $\mu = \mathcal{E}$ otherwise. This leads to the same upper bound in [11, (11) & (19)] as given in Theorem 3.

Next, we derive the rate achievable by using a truncated-Gaussian (TG) input distribution, and show that it is within a negligible gap of capacity at high SNR.

B. Truncated-Gaussian

We consider a distribution of X given by

$$\tilde{g}_{\mu,\nu}(x) = \eta g_{\mu,\nu}(x), \quad x \in [0, \mathcal{A}], \qquad (23)$$

for some $\mu \in \mathbb{R}$ and $\nu \in \mathbb{R}_+$, where $\eta = (G_{\mu,\nu}(\mathcal{A}) - G_{\mu,\nu}(0))^{-1}$. The mean of this distribution is

$$\tilde{\mu} = \int_0^{\mathcal{A}} x\tilde{g}_{\mu,\nu}(x)dx = \nu^2\eta(g_{\mu,\nu}(0) - g_{\mu,\nu}(\mathcal{A})) + \mu. \qquad (24)$$

We choose μ and ν such that $\tilde{\mu} \le \min\{\mathcal{E}, \frac{\mathcal{A}}{2}\}$ as stated in Theorem 4. For a given choice of μ and ν, the achievable rate can be expressed as $\mathcal{R} = I(X;Y)$ [25]. This mutual information is evaluated in Appendix D, leading to the achievable rate

$$\mathcal{R} = \mathcal{C}_0(\nu) - \Phi_1(\mu,\nu) - \Phi_2(\mu,\nu) - \Phi_3(\mu,\nu),$$

where $\mathcal{C}_0(\nu) = \frac{1}{2}\log\left(1+\frac{\nu^2}{\sigma^2}\right)$, $\Phi_1(\mu,\nu) = \log(\eta)$, $\Phi_2(\mu,\nu) = ((\mathcal{A}-\mu)g_{\mu,\nu}(\mathcal{A}) + \mu g_{\mu,\nu}(0))\frac{\eta\nu^2}{2(\nu^2+\sigma^2)}$, $\Phi_3(\mu,\nu) = \mathbb{E}_{X,Y}\left[\log(G_{\mu',\nu'}(\mathcal{A}) - G_{\mu',\nu'}(0))\right]$, $\mu' = \frac{\mu\sigma^2+y\nu^2}{\nu^2+\sigma^2}$, $\nu' = \frac{\nu\sigma}{\sqrt{\nu^2+\sigma^2}}$, and where the expectation is taken with respect to the distribution $f(x,y) = \eta g_{\mu,\nu}(x) g_{x,\sigma}(y)$.

Since $\Phi_3(\mu,\nu) < 0$, a more easily computable achievable rate can be obtained by dropping the term $\Phi_3(\mu,\nu)$ leading to

$$\mathcal{R}' = \mathcal{C}_0(\nu) - \Phi_1(\mu,\nu) - \Phi_2(\mu,\nu).$$

This achievable rate is close to capacity at high SNR (see Fig. 8). In particular, it is close to the sphere-packing bounds at high SNR. Interestingly, fixing $\mu = 0$ and optimizing with respect to ν suffices for approaching capacity at high SNR. Next, we simplify $\mathcal{R}'$ for the purpose of comparison with upper bounds at high SNR.

C. Simplification at High SNR

The achievable rate $\mathcal{R}'$ can be thought of as the sum of two quantities: the capacity of a Gaussian channel with Gaussian distributed input with variance ν^2 ($\mathcal{C}_0(\nu)$), and residual terms which arise due to the truncation of the Gaussian distribution.

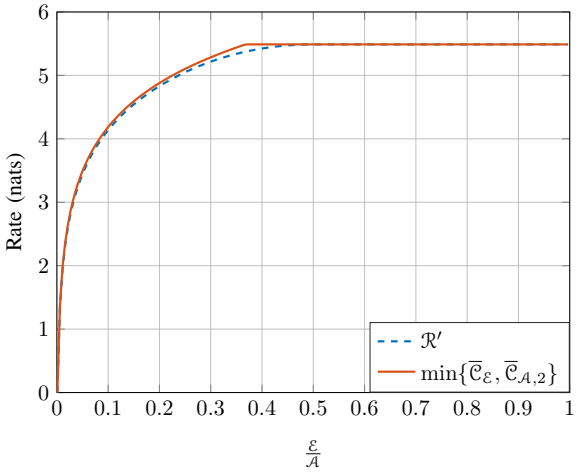

Fig. 8: Achievable rate of TG distribution and the sphere-packing upper bounds at $\mathcal{A}/\sigma = 30$dB versus $\frac{\mathcal{E}}{\mathcal{A}}$. Here, $\mathcal{R}'$ is obtained by fixing $\mu = 0$ and optimizing numerically with respect to ν.

With this interpretation, it is natural to check whether it is possible to make the residual terms vanish, leading to a simpler rate $\mathcal{R}' \approx \mathcal{C}_0(\nu)$.

Intuitively, the rate $\mathcal{C}_0(\nu)$ is achieved if the distributions $\tilde{g}_{\mu,\nu}(x)$ and $g_{\mu,\nu}(x)$ are almost identical. Thus, we need to choose μ and ν so that $G_{\mu,\nu}(0) \approx 0$ and $G_{\mu,\nu}(\mathcal{A}) \approx 1$. Since most of the mass of the Gaussian distribution $g_{\mu,\nu}(x)$ lies between $\mu - 3\nu$ and $\mu + 3\nu$, we choose $\mu = \min\left\{\frac{\mathcal{A}}{2}, \mathcal{E}\right\} - \xi$ and $\nu = \frac{\mu}{3}$, where ξ is a small quantity chosen so that $\tilde{\mu} \le \min\{\mathcal{E}, \frac{\mathcal{A}}{2}\}$ (24).

This choice leads to $\eta \le 1.0027$ with equality when $\mu = \mathcal{A}/2$, and thus $\Phi_1(\mu,\nu) \le 2.7\times10^{-3}$. On the other hand, this choice leads to $\mu g_{\mu,\nu}(0) = \frac{3}{e^4\sqrt{2e\pi}} \ge (\mathcal{A}-\mu)g_{\mu,\nu}(\mathcal{A})$ with equality if $\mu = \mathcal{A}/2$. Thus, $\Phi_2(\mu,\nu) \le \frac{3}{e^4\sqrt{2e\pi}}\frac{\eta\nu^2}{\nu^2+\sigma^2}$. For high SNR, $\Phi_1(\mu,\nu) + \Phi_2(\mu,\nu) < 0.016$ is negligible with respect to $\mathcal{C}_0(\nu)$. This leads to

$$\mathcal{R} \ge \mathcal{R}' > \mathcal{C}_0\left(\min\left\{\frac{\mathcal{A}}{2}, \mathcal{E}\right\}\right). \qquad (25)$$

If $\frac{\mathcal{E}}{\mathcal{A}} < \frac{1}{2}$, then the achievable rate (25) becomes $\frac{1}{2}\log\left(\frac{\bar{\gamma}^2}{9}\right)$ at high SNR. This achievable rate is within < 0.68 nats of the upper bound $\overline{\mathcal{C}}_{\mathcal{E}}$ (Theorem 2) at high SNR. Otherwise, if $\frac{\mathcal{E}}{\mathcal{A}} \ge \frac{1}{2}$, then the achievable rate (25) is $\frac{1}{2}\log\left(\frac{\gamma^2}{36}\right)$, which is within < 0.38 nats of the upper bound $\overline{\mathcal{C}}_{\mathcal{A},2}$ (Theorem 1).

Although the bound (25) is simple, and is within a constant of capacity at high SNR, it is not as close to capacity as one desires. Table I gives selections of μ and ν that bring $\mathcal{R}'$ closer to capacity at high SNR. The calculation of the gap $\min\{\overline{\mathcal{C}}_{\mathcal{E}}, \overline{\mathcal{C}}_{\mathcal{A},2}\} - \mathcal{R}'$ for $\frac{\mathcal{E}}{\mathcal{A}} \in \left(0, \sqrt{\frac{2}{9\pi}}\right]$ is given in Appendix E. The gap for the other cases can be obtained similarly.

By maximizing numerically with respect to μ and ν, the gap to the sphere-packing bounds at high SNR can be sharpened to < 0.1 nats as shown in Fig. 2. Furthermore, by incorporating the upper bound $\overline{\mathcal{C}}_{L,1}$ given in [11, (12)] into the comparison, the gap $\Delta' = \min\{\overline{\mathcal{C}}_{\mathcal{E}}, \overline{\mathcal{C}}_{\mathcal{A},2}, \overline{\mathcal{C}}_{L,1}\} - \mathcal{R}'$ reduces to ≈ 0 at high

This article has been accepted for publication in a future issue of this journal, but has not been fully edited. Content may change prior to final publication. Citation information: DOI 10.1109/TCOMM.2016.2524569, IEEE Transactions on Communications

$\frac{\mathcal{E}}{\mathcal{A}}$	$\left(0, \sqrt{\frac{2}{9\pi}}\right]$	$\left(\sqrt{\frac{2}{9\pi}}, \frac{1}{3.2}\right]$	$\left(\frac{1}{3.2}, \frac{1}{e}\right]$	$\left(\frac{1}{e}, \frac{1}{2}\right)$	$\frac{1}{2}$
μ	0	0	0	$\frac{\mathcal{A}}{4}$	$\frac{\mathcal{A}}{2}$
ν	$\sqrt{\frac{\pi}{2}\mathcal{E}}$	$\sqrt{\frac{\pi}{2}\mathcal{E}}$	$\sqrt{\frac{\pi}{2}\mathcal{E}}$	$\frac{\mathcal{A}}{3}$	$\mathcal{A}$
$\min\{\overline{\mathcal{C}}_{\mathcal{E}}, \overline{\mathcal{C}}_{\mathcal{A},2}\} - \mathcal{R}'$	< 0.062	< 0.099	< 0.163	< 0.144	≈ 0

TABLE I: Selections of μ and ν that lead to $\mathcal{R}'$ close to capacity at high SNR.

SNR. Based on these numerical observations, we conclude that the TG input distribution is nearly capacity achieving at high SNR.

Since we are interested in simple capacity expressions, we approximate the high-SNR capacity by

$$\begin{aligned}\mathcal{C}_{\text{high SNR}} &\approx \lim_{\gamma\to\infty} \min\{\overline{\mathcal{C}}_{\mathcal{E}}, \overline{\mathcal{C}}_{\mathcal{A},2}\} \\ &= \min\left\{\frac{1}{2}\log\left(\frac{e\bar{\gamma}^2}{2\pi}\right), \frac{1}{2}\log\left(\frac{\gamma^2}{2\pi e}\right)\right\},\end{aligned}$$

as in Proposition 1. This approximation is exact for $\frac{\mathcal{E}}{\mathcal{A}} > \frac{1}{2}$ at high SNR where the lower bound [11, (18)] coincides with $\overline{\mathcal{C}}_{\mathcal{A},2}$. This approximation is nearly tight (≈ 0 gap to capacity) for $\frac{\mathcal{E}}{\mathcal{A}} \leq 0.15$ where $\mathcal{R}'$ approaches $\overline{\mathcal{C}}_{\mathcal{E}}$ (see Fig. 2a). For $0.15 < \frac{\mathcal{E}}{\mathcal{A}} \leq \frac{1}{2}$, the approximation is fairly tight since the gap is < 0.1 nats and can be neglected at high SNR.

VII. Capacity Fitting

It is of practical interest to have a closed-form expression which captures the achievable rate $\mathcal{R}_F$ in [12]. Such an expression can be used to study power allocation and outage/ergodic capacities of fading scenarios. While such a closed form expression is given for high SNR by Proposition 1, and for low SNR by [11], it is not available for moderate SNR; the regime of operation of practical systems. With this in mind, we provide simple expressions for the achievable rate in an IM-DD channel using curve-fitting. We first present a global fitting for $\mathcal{R}_F$ for all SNR.

A. Global Fitting

We need to choose a fitting that captures the behavior of $\mathcal{R}_F$ [12] from low to high SNR. Let the fitting function be denoted $\Psi(\gamma)$. As discussed in the previous section, the high SNR capacity of the channel scales as $\frac{1}{2}\log(c_1\gamma^2)$ for some $c_1 > 0$. On the other hand, the low SNR capacity scales as $c_2\frac{\gamma^2}{2}$ [11] for some $c_2 > 0$. A suitable fitting for high and low γ is thus given by the function $\Psi(\gamma) = \frac{1}{2}\log\left(1 + \gamma^2(c_1 + (c_2 - c_1)\Theta(\gamma))\right)$, where $\Theta(\gamma)$ is a function which satisfies $\lim_{\gamma\to\infty}\Theta(\gamma) = 0$ and $\lim_{\gamma\to 0}\Theta(\gamma) = 1$. By choosing c_1 and c_2 appropriately, $\Psi(\gamma)$ captures the high and low SNR behavior of capacity. It remains to capture $\mathcal{R}_F$ in the moderate SNR regime (see Figure 3). To this end, we have to choose $\Theta(\gamma)$ appropriately. A convenient choice is of the form of a $\Theta(\gamma) = \frac{\Theta_1(\gamma)}{\Theta_2(\gamma)}$, where $\Theta_1(\gamma)$ and $\Theta_2(\gamma)$ are polynomials of degrees m_1 and $m_2 > m_1$ in γ, respectively. That is,

$$\Psi(\gamma) = \frac{1}{2}\log\left(1 + \gamma^2\left(c_1 + (c_2 - c_1)\frac{\sum_{k=0}^{m_1} a_k\gamma^k}{\sum_{k=0}^{m_2} b_k\gamma^k}\right)\right),$$

for some c_1, c_2, a_k and b_k to be determined. Without loss of generality, we fix $a_0 = b_0 = 1$. The remaining coefficients of $\Theta_1(\gamma)$ and $\Theta_2(\gamma)$ have to be chosen so that these polynomials have no roots in $[0, \infty)$ to avoid singularities. The parameters c_1 and c_2 can be easily fixed using our knowledge of the high and low SNR capacity of the channel. Namely,

$$c_1 = \min\left\{\frac{e\bar{\gamma}^2}{2\pi\gamma^2}, \frac{1}{2\pi e}\right\}, \tag{26}$$

$$c_2 = \min\left\{\frac{\bar{\gamma}}{\gamma}\left(1 - \frac{\bar{\gamma}}{\gamma}\right), \frac{1}{4}\right\}. \tag{27}$$

The parameters m_1 and m_2 can be chosen based on the number of SNR-Rate pairs (γ, R) used for the fitting in the moderate SNR regime. In particular, given N_p such pairs $\{(\gamma_1, R_1), \cdots, (\gamma_{N_p}, R_{N_p})\}$, we can choose $m_2 = \left\lceil\frac{N_p+1}{2}\right\rceil$ and $m_1 = N_p - m_2$. This guarantees that $m_1 < m_2$ and that the number of unknown parameters of the fitting function $\Psi(\gamma)$ does not exceed N_p. After fixing m_1 and m_2, the parameters a_k and b_k can be easily chosen by solving the linear system of equations

$$\sum_{k=0}^{m_1} a_k\gamma_i^k - \left(\frac{e^{2R_i} - 1 - c_1\gamma_i^2}{(c_2 - c_1)\gamma_i^2}\right)\sum_{k=0}^{m_2} b_k\gamma_i^k = 0, \tag{28}$$

$i = 1, \cdots, N_p$. Thus, by choosing m_1 and m_2 as described above, we have N_p equations with N_p unknowns and we can solve for the parameters a_k and b_k. Recall that we obtain the SNR-Rate pairs from $\mathcal{R}_F$ [12].

By numerical inspection, a very close fit can be obtained for $N_p \leq 3$ (see Fig. 9). By using $N_p = 1$ and $N_p = 3$, we get $(m_1, m_2) = (0, 1)$ and $(m_1, m_2) = (1, 2)$. While the latter gives a very close fit, the former gives a simpler fitting at the expense of a small gap. The coefficients of the fitting functions are summarized in Table II for different values of $\frac{\mathcal{E}}{\mathcal{A}}$. For the five cases in this table, the polynomials $\Theta_1(\gamma)$ and $\Theta_2(\gamma)$ have no roots in $[0, \infty)$. Notice that the achievable rate (as a function of γ) of an IM-DD channel with a given $\frac{\mathcal{E}}{\mathcal{A}}$ is also achievable for any channel with larger $\frac{\mathcal{E}}{\mathcal{A}}$, since the latter has larger average constraint. Thus, by plugging the coefficients given in Table II for $\frac{\mathcal{E}}{\mathcal{A}} = \alpha$ in $\Psi(\gamma)$, we obtain achievable rates for an IM-DD with $\frac{\mathcal{E}}{\mathcal{A}} > \alpha$ as well. The values in the table can be used for studying the performance of fading IM-DD channels at any SNR.

B. Local Fitting

The function $\Psi(\gamma)$ is a close fit for all SNR. However, in practice, we are often interested in functions of the form $\frac{1}{2}\log(1 + c\gamma^2)$, especially since numerous techniques have been developed over the time to study capacity of this form in fading scenarios (power allocation, outage, etc.) [31], [32].

This article has been accepted for publication in a future issue of this journal, but has not been fully edited. Content may change prior to final publication. Citation information: DOI 10.1109/TCOMM.2016.2524569, IEEE Transactions on Communications

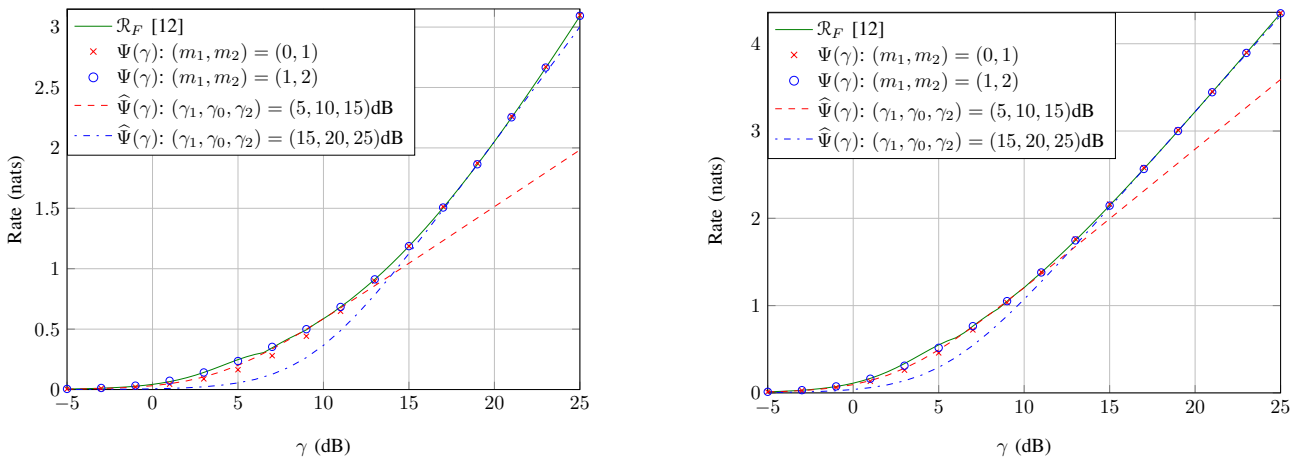

(a) $\frac{\mathcal{E}}{\mathcal{A}} = 0.1$. (b) $\frac{\mathcal{E}}{\mathcal{A}} = \frac{1}{2}$.

Fig. 9: Global and local fitting of the achievable rate $\mathcal{R}_F$ using $\Psi(\gamma)$ and $\widehat{\Psi}(\gamma)$.

$\frac{\mathcal{E}}{\mathcal{A}}$		0.1	0.2	0.3	0.4	0.5
$N_p = 1$	a_0 (b_0, b_1)	1 $(1, 0.47)$	1 $(1, 0.43)$	1 $(1, 0.56)$	1 $(1, 0.8)$	1 $(1, 0.41)$
$N_p = 3$	(a_0, a_1) (b_0, b_1, b_2)	$(1, 0.38)$ $(1, 0.19, 0.2)$	$(1, 0.45)$ $(1, 0.24, 0.21)$	$(1, 0.14)$ $(1, 0.04, 0.1)$	$(1, 0.05)$ $(1, -0.03, 0.07)$	$(1, 0.57)$ $(1, 0.32, 0.26)$

TABLE II: Coefficients of the fitting function $\Psi(\gamma)$ using one fitting point at $\gamma = 15$ dB and three fitting points at $\gamma \in \{0, 10, 15\}$ dB.

Thus, it is natural to seek a fitting function of this form. Next, we simplify the fitting function $\Psi(\gamma)$ to this form by sacrificing its global tightness.

As evident from Fig. 3 e.g., the lower bound $\mathcal{R}_F$ can not be captured by a function of the form $\frac{1}{2}\log(1 + c\gamma^2)$ in the moderate γ regime since this function has a larger pre-log. However, a local fit can be obtained by using a rather simple fitting function

$$\widehat{\Psi}(\gamma) = \frac{d_1}{2}\log(1 + d_2\gamma^2),$$

where d_1 and d_2 are positive scalars. At high γ, $d_1 = 1$ and $d_2 = c_1$ given in (26). At low γ, we can choose any d_1 and d_2 such that $d_1 d_2 = c_2$ given in (27). For moderate SNR, d_1 and d_2 have to be chosen to reduce the gap between $\widehat{\Psi}(\gamma)$ and the achievable rate $\mathcal{R}_F$ for an SNR range of interest. It is also important to maintain $\hat{\Psi}(\gamma) < \mathcal{R}_F$ to guarantee that $\hat{\Psi}(\gamma)$ is achievable. Next, we propose a simple method to obtain a local fit for moderate γ.

Consider an SNR range of interest $\gamma \in [\gamma_1, \gamma_2]$ dB for some γ_1 and γ_2, and consider the achievable rates R_1, R_2, and R_0 corresponding to $\mathcal{R}_F$ in [12] at γ_1, γ_2, and some $\gamma_0 \in [\gamma_1, \gamma_2]$, respectively. First, we choose d_1 as the pre-log of $\mathcal{R}_F$ (slope with respect to $\log(\gamma)$) in this range of γ, i.e., $d_1 = \frac{R_2 - R_1}{\log(\gamma_2) - \log(\gamma_1)}$. Roughly, this indicates that the achievable rate $\mathcal{R}_F$ scales as $\frac{d_1}{2}\log(\gamma^2)$ in this range. Now, to fix d_2, we equate $\widehat{\Psi}(\gamma_0)$ to R_0, leading to $d_2 = \frac{e^{\frac{2R_0}{d_1}} - 1}{\gamma_0^2}$.

Alternatively, one could use an MMSE approach to minimize the gap between $\hat{\Psi}(\gamma)$ and $\mathcal{R}_F$. We repeat that $\widehat{\Psi}(\gamma)$ provides local fitting, contrary to $\Psi(\gamma)$. The behavior of $\widehat{\Psi}(\gamma)$ is depicted in Figure 9. Note that $\widehat{\Psi}(\gamma)$ provides a good fit for the range of interest. The advantage of this function is that it has a simple form that can be used for studying fading scenarios using existing tools. In scenarios with weak turbulence conditions e.g., the SNR γ does not vary widely resulting in a distribution of γ that is thin around a nominal value γ_0. The performance of a system operating around γ_0 can be well described by $\widehat{\Psi}(\gamma)$ in the given range.

VIII. Conclusion

We studied a simple model of the IM-DD channel with input-independent noise. For this model, we proposed a new approach for deriving sphere-packing upper bounds. The proposed recursive approach is better than the approach that uses the Steiner-Minkowski formula which is commonly used in literature. The main reason is that our approach makes use of the geometry of the ball, while the other approach does not. This recursive approach can in fact be applied to any scenario where the input signal of the channel is confined to a polyhedron. The resulting bounds are tighter than existing bounds in some SNR regimes. An interesting extension of these sphere-packing bounds would be to generalize them to the intersection of a cube and a simplex, which better captures the IM-DD channel under both average and peak intensity constraints. We also derived the rate achieved by using a truncated-Gaussian input distribution. By comparing with the upper bounds, we show that the gap between the achievable rate and upper bounds is negligible at high SNR. We also provide simple functions that describe the highest known achievable rate of this channel globally and locally.

This article has been accepted for publication in a future issue of this journal, but has not been fully edited. Content may change prior to final publication. Citation information: DOI 10.1109/TCOMM.2016.2524569, IEEE Transactions on Communications

Such function can be of great importance for studying fading in practical systems.

ACKNOWLEDGEMENT

The authors are grateful to Dr. Zouheir Rezki, and to the editor and reviewers. Their insightful comments significantly improved this paper.

APPENDIX A
SUFFICIENCY OF $\mathbb{E}[X] = \min\{\mathcal{E}, \frac{\mathcal{A}}{2}\}$

For an IM-DD channel with input-independent noise, the capacity achieving input distribution satisfies $\mathbb{E}[X] = \min\{\mathcal{E}, \frac{\mathcal{A}}{2}\}$. The proof is simple for a channel with an average constraint only ($\mathcal{A} = \infty$), where it follows from the invariance of mutual information to shifts in the input distribution. That is, we can always shift X to obtain a distribution with a larger mean achieving the same rate. This proof is however not possible for $X \in [0, \mathcal{A}]$ since shifting might lead to an infeasible distribution. Instead, we show that over the set of distributions of $X \in [0, \mathcal{A}]$, $\mathcal{C}$ is increasing in $\mathbb{E}[X]$ for $\mathbb{E}[X] \in (0, \frac{\mathcal{A}}{2}]$, and decreasing for $\mathbb{E}[X] \in (\frac{\mathcal{A}}{2}, \mathcal{A}]$.

The proof is similar to [11, Proposition 9]. Consider a peak constrained IM-DD channel, and input distributions $f_1(x)$ and $f_2(x) = f_1(\mathcal{A} - x)$ on $X \in [0, \mathcal{A}]$ with means $\mu_1 \leq \frac{\mathcal{A}}{2}$ and $\mu_2 \geq \frac{\mathcal{A}}{2}$, respectively. Denote the rates achieved by these distributions by I_1 and I_2, respectively. Since $f_2(x) = f_1(\mathcal{A} - x)$, and due to the symmetry of the Gaussian noise distribution around 0, we have $I_1 = I_2$. Consider now the mixture of the two distributions $f_3(x) = \tau f_1(x) + (1-\tau) f_2(x)$, $\tau \in [0, 1]$, which has the same support and has mean $\mu_3 = \tau\mu_1 + (1-\tau)\mu_2 \in [\mu_1, \mu_2]$. By Jensen's inequality and the concavity of the mutual information in $f(x)$ for a given $f(y|x)$ [25], we have

$$I(X;Y)|_{f_3(x)} = I_3 \geq \tau I_1 + (1-\tau) I_2 = I_1,$$

with equality if $\tau = 1$ or $\tau = 0$. Thus, for any $\mu_1 \leq \frac{\mathcal{A}}{2}$ (or $\mu_2 \geq \frac{\mathcal{A}}{2}$), there exists a distribution with mean $\mu_3 \geq \mu_1$ (or $\mu_3 \leq \mu_2$) which achieves higher rate. Therefore, $\mathcal{C}$ is increasing in $\mathbb{E}[X] \in (0, \frac{\mathcal{A}}{2}]$, and decreasing in $\mathbb{E}[X] \in (\frac{\mathcal{A}}{2}, \mathcal{A}]$, which proves that the optimal distribution has $\mathbb{E}[X] = \min\{\mathcal{E}, \frac{\mathcal{A}}{2}\}$.

APPENDIX B
BOUNDING THE LIMIT IN (3)

Here, we upper bound $\lim_{n\to\infty} \frac{1}{n} \log\left(\sum_{i=0}^{n} N_i\right)$ where $N_i = \binom{n}{n-i} \left(\frac{\mathcal{A}}{\sqrt{\pi n \sigma^2}}\right)^{n-i} \frac{\Gamma\left(1+\frac{n}{2}\right)}{\Gamma\left(1+\frac{i}{2}\right)}$, using similar steps as [13]. We start by writing

$$N_i = \left(\frac{\mathcal{A}}{\sqrt{\pi n \sigma^2}}\right)^{n-i} \frac{\Gamma\left(1+\frac{n}{2}\right)\Gamma\left(1+n\right)}{\Gamma\left(1+\frac{i}{2}\right)\Gamma\left(1+n-i\right)\Gamma\left(1+i\right)}$$

using the definition of the binomial coefficient and the Gamma function [33]. Note that

$$\begin{aligned}\frac{1}{n}\log\left(\sup_{i\in\{0,\cdots,n\}} N_i\right) &\leq \frac{1}{n}\log\left(\sum_{i=0}^{n} N_i\right) \\ &\leq \frac{1}{n}\log\left((n+1)\sup_{i\in\{0,\cdots,n\}} N_i\right)\end{aligned}$$

and that

$$\lim_{n\to\infty}\frac{1}{n}\log\left(\sup_{i\in\{0,\cdots,n\}} N_i\right) = \lim_{n\to\infty}\frac{1}{n}\log\left((n+1)\sup_{i\in\{0,\cdots,n\}} N_i\right).$$

Thus

$$\begin{aligned}\lim_{n\to\infty}\frac{1}{n}\log\left(\sum_{i=0}^{n} N_i\right) &= \lim_{n\to\infty}\frac{1}{n}\log\left(\sup_{i\in\{0,\cdots,n\}} N_i\right) \\ &= \lim_{n\to\infty}\sup_{i\in\{0,\cdots,n\}}\frac{1}{n}\log\left(N_i\right) \\ &\leq \lim_{n\to\infty}\sup_{\alpha\in[0,1]}\frac{1}{n}\log\left(N_{\alpha n}\right),\end{aligned}$$

where the second step follows by the monotonicity of the logarithm, and the third by replacing $i \in \{0, \cdots, n\}$ by αn with $\alpha \in [0, 1]$. Using Stirling's bound [34] $\sqrt{2\pi n}\left(\frac{n}{e}\right)^n e^{\frac{1}{12n+1}} \leq \Gamma(n+1) \leq \sqrt{2\pi n}\left(\frac{n}{e}\right)^n e^{\frac{1}{12n}}$, and after some manipulation, we obtain

$$N_{\alpha n} \leq \left[\left(\frac{\mathcal{A}^2}{2\pi e\sigma^2}\right)^{\frac{1-\alpha}{2}} \alpha^{-\frac{3\alpha}{2}}(1-\alpha)^{\alpha-1}\right]^n \frac{e^{\frac{1}{4n}}}{\alpha\sqrt{2\pi n(1-\alpha)}}.$$

The limit $\lim_{n\to\infty}\frac{1}{n}\log\left(N_{\alpha n}\right)$ exists, and is equal to $B_1'(\alpha) = (1-\alpha)\log\left(\frac{\gamma}{\sqrt{2\pi e}}\right) - \log\left((1-\alpha)^{1-\alpha}\alpha^{\frac{3\alpha}{2}}\right)$. Thus, we can exchange the lim and the sup leading to $\lim_{n\to\infty}\frac{1}{n}\log\left(\sum_{i=0}^{n} N_i\right) \leq \sup_{\alpha\in[0,1]} B_1'(\alpha)$. Now by replacing α by $1-\alpha$, we obtain $B_1(\alpha)$ and the the upper bound $\overline{\mathcal{C}}_{\mathcal{A},1}$ given in Theorem 1.

APPENDIX C
BOUNDING THE EQUIVALENT HEIGHT OF A SPHERICAL-CAP

The volume of a spherical-cap of radius λ and height $h \in [0, \lambda]$ is [35]

$$V(\mathcal{P}_{\lambda,h}^n) = \frac{1}{2}V(\mathcal{B}_\lambda^n) I_{\frac{\lambda'^2}{\lambda^2}}\left(\frac{n+1}{2}, \frac{1}{2}\right), \tag{29}$$

where $\lambda' = \sqrt{2h\lambda - h^2}$, and $I_x(a,b)$ is the regularized incomplete beta function. The base of this spherical-cap is $\mathcal{B}_{\lambda'}^{n-1}$. Thus, the height of the equivalent cylinder is

$$\begin{aligned}h' &= \frac{1}{2}\frac{V(\mathcal{B}_\lambda^n)}{V(\mathcal{B}_{\lambda'}^{n-1})} I_{\frac{\lambda'^2}{\lambda^2}}\left(\frac{n+1}{2}, \frac{1}{2}\right) &(30)\\ &= \hat{h}_n \frac{V(\mathcal{B}_\lambda^{n-1})}{V(\mathcal{B}_{\lambda'}^{n-1})} I_{\frac{\lambda'^2}{\lambda^2}}\left(\frac{n+1}{2}, \frac{1}{2}\right), &(31)\end{aligned}$$

where $\hat{h}_n = \frac{V(\mathcal{B}_\lambda^n)}{2V(\mathcal{B}_\lambda^{n-1})}$. Thus,

$$h' = \hat{h}_n \left(\frac{\lambda^2}{\lambda'^2}\right)^{\frac{n-1}{2}} I_{\frac{\lambda'^2}{\lambda^2}}\left(\frac{n+1}{2}, \frac{1}{2}\right).$$

This article has been accepted for publication in a future issue of this journal, but has not been fully edited. Content may change prior to final publication. Citation information: DOI 10.1109/TCOMM.2016.2524569, IEEE Transactions on Communications

Using the identity $I_x(a,b) = \frac{x^a F(a,1-b;a+1;x)}{F(a,1-b;a+1;1)}$ [33, Sec. 6.6] where $F(a,b;c;x)$ is the Gauss hypergeometric function, we can write

$$h' = \hat{h}_n \left(\frac{\lambda^2}{\lambda'^2}\right)^{\frac{n-1}{2}} \frac{\left(\frac{\lambda'^2}{\lambda^2}\right)^{\frac{n+1}{2}} F\left(\frac{n+1}{2}, \frac{1}{2}; \frac{n+3}{2}; \frac{\lambda'^2}{\lambda^2}\right)}{F\left(\frac{n+1}{2}, \frac{1}{2}; \frac{n+3}{2}; 1\right)}$$
$$= \hat{h}_n \underbrace{\left(\frac{\lambda'^2}{\lambda^2}\right) \frac{F\left(\frac{n+1}{2}, \frac{1}{2}; \frac{n+3}{2}; \frac{\lambda'^2}{\lambda^2}\right)}{F\left(\frac{n+1}{2}, \frac{1}{2}; \frac{n+3}{2}; 1\right)}}_{f(\lambda')}.$$

But since $h \in [0,\lambda]$, then $\lambda' \in [0,\lambda]$. Furthermore, $\frac{\lambda'^2}{\lambda^2}$ and $F\left(\frac{n+1}{2}, \frac{1}{2}; \frac{n+3}{2}; \frac{\lambda'^2}{\lambda^2}\right)$ are both increasing in λ', and hence, $f(\lambda')$ is increasing in λ'. Since $f(0) = 0$ and $f(\lambda) = 1$, it follows that $h' \leq \hat{h}_n$.

Appendix D
Derivation of the Lower Bound in Section VI-B

We start by writing the achievable rate $R = I(X;Y)$ with input distribution $\tilde{g}_{\mu,\sigma}(x)$ described in (23) as

$$\mathcal{R} = \int_0^{\mathcal{A}} \int_{-\infty}^{\infty} f(x,y) \log\left(\frac{f(y|x)}{f(y)}\right) dydx \tag{32}$$
$$= \int_0^{\mathcal{A}} \int_{-\infty}^{\infty} f(x,y) \log\left(f(y|x)\right) dydx - \int_0^{\mathcal{A}} \int_{-\infty}^{\infty} f(x,y) \log\left(f(y)\right) dydx. \tag{33}$$

The first integral above is -1 times the entropy of noise. Hence it is equal to

$$T_0 = \int_0^{\mathcal{A}} \int_{-\infty}^{\infty} f(x,y) \log\left(f(y|x)\right) dydx = -\frac{1}{2}\log(2\pi e\sigma^2). \tag{34}$$

Next, we substitute $f(y) = \eta g_{\mu_0,\sigma_y}(y)(G_{\mu',\nu'}(\mathcal{A}) - G_{\mu',\nu'}(0))$ in the second integral to obtain

$$T = \int_0^{\mathcal{A}} \int_{-\infty}^{\infty} f(x,y) \log\left(\eta\right) dydx + \int_0^{\mathcal{A}} \int_{-\infty}^{\infty} f(x,y) \log\left(g_{\mu_0,\sigma_y}(y)\right) dydx + \int_0^{\mathcal{A}} \int_{-\infty}^{\infty} f(x,y) \log\left(G_{\mu',\nu'}(\mathcal{A}) - G_{\mu',\nu'}(0)\right) dydx$$
$$= T_1 + T_2 + T_3, \tag{35}$$

where T_1, T_2, and T_3 denote the three integrals above, respectively. The first term T_1 is clearly $T_1 = \log(\eta)$. The last term T_3 can be written as $T_3 = \mathbb{E}_{X,Y}[\log\left(G_{\mu',\nu'}(\mathcal{A}) - G_{\mu',\nu'}(0)\right)]$ where the expectation is with respect to the distribution $f(x,y)$. It remains to evaluate T_2 in order to obtain the achievable rate $\mathcal{R}$ in Theorem 4. We start by substituting $g_{\mu,\sigma_y}(y)$ in T_2, yielding

$$T_2 = \int_0^{\mathcal{A}} \int_{-\infty}^{\infty} f(x,y) \log\left(\sqrt{\frac{1}{2\pi\sigma_y^2}}\right) dydx + \int_0^{\mathcal{A}} \int_{-\infty}^{\infty} f(x,y) \left(-\frac{(y-\mu)^2}{2\sigma_y^2}\right) dydx \tag{36}$$
$$= -\frac{1}{2}\log\left(2\pi\sigma_y^2\right) - \frac{1}{2\sigma_y^2}\int_0^{\mathcal{A}} \mathbb{E}_{Y|X}\left[Y^2\right] \tilde{g}_{\mu,\nu}(x)dx - \frac{1}{2\sigma_y^2}\int_0^{\mathcal{A}} \left(-2\mu\mathbb{E}_{Y|X}\left[Y\right] + \mu^2\right) \tilde{g}_{\mu,\nu}(x)dx \tag{37}$$
$$= -\frac{1}{2}\log\left(2\pi\sigma_y^2\right) - \frac{\sigma^2}{2\sigma_y^2} - \frac{1}{2\sigma_y^2}\int_0^{\mathcal{A}} (x-\mu)^2 \tilde{g}_{\mu,\nu}(x)dx$$
$$= -\frac{1}{2}\log\left(2\pi\sigma_y^2\right) - \frac{\sigma^2}{2\sigma_y^2} - \frac{1}{2\sigma_y^2}\mathbb{E}_X[(X-\mu)^2]. \tag{38}$$

Finally, we evaluate the expectation $\mathbb{E}_X[(X-\mu)^2]$ as follows

$$\mathbb{E}_X[(X-\mu)^2] = \eta\frac{2\nu^2}{\sqrt{\pi}} \int_{-\frac{\mu}{\sqrt{2}\nu}}^{\frac{\mathcal{A}-\mu}{\sqrt{2}\nu}} t^2 e^{-t^2} dt \tag{39}$$
$$= \eta\frac{\nu^2}{\sqrt{\pi}} \left(\int_{-\frac{\mu}{\sqrt{2}\nu}}^{\frac{\mathcal{A}-\mu}{\sqrt{2}\nu}} e^{-t^2} dt - \left[te^{-t^2}\right]_{-\frac{\mu}{\sqrt{2}\nu}}^{\frac{\mathcal{A}-\mu}{\sqrt{2}\nu}}\right)$$
$$= \nu^2 \left[\int_0^{\mathcal{A}} \tilde{g}_{\mu,\nu}(x)dx - (\mathcal{A}-\mu)\tilde{g}_{\mu,\nu}(\mathcal{A}) - \mu\tilde{g}_{\mu,\nu}(0)\right]$$
$$= \nu^2\left(1 - (\mathcal{A}-\mu)\tilde{g}_{\mu,\nu}(\mathcal{A}) - \mu\tilde{g}_{\mu,\nu}(0)\right). \tag{40}$$

Collecting the terms T_0, T_1, T_2, and T_3, and substituting in (33), yields the desired expression

$$\mathcal{R} = \frac{1}{2}\log\left(1 + \frac{\nu^2}{\sigma^2}\right) - \log(\eta) - \left((\mathcal{A}-\mu)\tilde{g}_{\mu,\nu}(\mathcal{A}) + \mu\tilde{g}_{\mu,\nu}(0)\right)\frac{\nu^2}{2(\nu^2+\sigma^2)} - \mathbb{E}_{X,Y}\left[\log(G_{\mu',\nu'}(\mathcal{A}) - G_{\mu',\nu'}(0))\right],$$

where we replaced σ_y^2 by its value $\sigma^2 + \nu^2$. This completes the proof of Theorem 4.

Note that since $\eta > 1$, then $T_1 = \log(\eta)$ can be considered as a penalty arising due to the truncation of the Gaussian distribution, which reduces the rate below $\frac{1}{2}\log\left(1 + \frac{\nu^2}{\sigma^2}\right)$. The second term T_2 can be positive or negative depending on the choice of μ and ν. The last term T_3 is always negative, and hence it always increases the achievable rate. Since this term might be difficult to compute, and since it is always negative, we can drop it an obtain the achievable rate $\mathcal{R}'$ as given in Theorem 4.

This article has been accepted for publication in a future issue of this journal, but has not been fully edited. Content may change prior to final publication. Citation information: DOI 10.1109/TCOMM.2016.2524569, IEEE Transactions on Communications

APPENDIX E
GAP BETWEEN $\mathcal{R}'$ AND SPHERE-PACKING BOUNDS FOR SELECTIONS OF μ AND ν

Recall that the achievable rate $\mathcal{R}'$ is given by

$$\mathcal{R}' = \frac{1}{2}\log\left(1+\frac{\nu^2}{\sigma^2}\right) - \log(\eta) - \left((\mathcal{A}-\mu)g_{\mu,\nu}(\mathcal{A}) + \mu g_{\mu,\nu}(0)\right)\frac{\eta\nu^2}{2(\nu^2+\sigma^2)},$$

where $\eta = \frac{1}{G_{\mu,\nu}(\mathcal{A})-G_{\mu,\nu}(0)}$, and μ and ν are chosen such that $\tilde{\mu} = \nu^2\eta(g_{\mu,\nu}(0) - g_{\mu,\nu}(\mathcal{A})) + \mu \leq \mathcal{E}$.

Let us fix $\mu = 0$ and $\nu = \sqrt{\frac{\pi}{2}}\mathcal{E}$. To simplify the computation, we would like to have $G_{\mu,\nu}(\mathcal{A}) \approx 1$, which can be achieved if $\nu \leq \frac{\mathcal{A}}{3}$ leading to the constraint $\mathcal{E} \leq \frac{\mathcal{A}}{3}\sqrt{\frac{2}{\pi}}$. Using this selection for $\mathcal{E} \in \left(0, \frac{\mathcal{A}}{3}\sqrt{\frac{2}{\pi}}\right]$, we have $G_{\mu,\nu}(\mathcal{A}) \approx 1$, $G_{\mu,\nu}(0) = \frac{1}{2}$, $g_{\mu,\nu}(\mathcal{A}) < \frac{1}{\pi\mathcal{E}}e^{-\frac{\mathcal{A}^2}{\pi\mathcal{E}^2}}$, $g_{\mu,\nu}(0) = \frac{1}{\pi\mathcal{E}}$. This leads to $\eta \approx 2$ and $\tilde{\mu} < \mathcal{E}$. The achievable rate is given by

$$\begin{aligned}\mathcal{R}' &= \frac{1}{2}\log\left(1+\frac{\pi\mathcal{E}^2}{2\sigma^2}\right) - \log(2) - \mathcal{A}g_{\mu,\nu}(\mathcal{A})\frac{\nu^2}{\nu^2+\sigma^2} \\ &> \frac{1}{2}\log\left(\pi\mathcal{E}^2/(8\sigma^2)\right) - \mathcal{A}g_{\mu,\nu}(\mathcal{A}).\end{aligned}$$

But $\mathcal{A}g_{\mu,\nu}(\mathcal{A}) < \frac{\mathcal{A}}{\pi\mathcal{E}}e^{-\frac{\mathcal{A}^2}{\pi\mathcal{E}^2}} = \frac{1}{\sqrt{\pi}}te^{-t^2}$ where $t = \frac{\mathcal{A}}{\sqrt{\pi}\mathcal{E}}$. Also, for $\mathcal{E} \leq \frac{\mathcal{A}}{3}\sqrt{\frac{2}{\pi}}$, we have $t > \frac{3}{\sqrt{2}} > \frac{1}{\sqrt{2}}$. Since the function te^{-t^2} is decreasing for $t > \frac{1}{\sqrt{2}}$, then $\mathcal{A}g_{\mu,\nu}(\mathcal{A}) < \frac{1}{\sqrt{\pi}}\frac{3}{\sqrt{2}}e^{-\frac{9}{2}} < 0.0133$. Therefore, at high SNR where the sphere packing bound $\overline{\mathcal{C}}_{\mathcal{E}}$ becomes $\frac{1}{2}\log\left(\frac{e\mathcal{E}^2}{2\pi\sigma^2}\right)$ the gap can be bounded as

$$\overline{\mathcal{C}}_{\mathcal{E}} - \mathcal{R}' < \frac{1}{2}\log\left(\frac{e}{2\pi}\frac{8}{\pi}\right) + 0.0133 < 0.062.$$

Similar analysis can be applied to all other cases leading to the values given in Table I.

REFERENCES

[1] A. Chaaban, J.-M. Morvan, and M. S. Alouini, "Free-space optical communications with peak and average constraints: High SNR capacity approximation," in *4th International Workshop on Optical Wireless Communications (IWOW)*, Sept 2015, pp. 73–77.

[2] J. Akella, M. Yuksel, and S. Kalyanaraman, "Error analysis of multi-hop free-space optical communications," in *Proc. of IEEE International Conference on Communications (ICC)*, May. 2005, pp. 1777–1781.

[3] S. Kazemlou, S. Hranilovic, and S. Kumar, "All-optical multihop free-space optical communication systems," *Journal of Lightwave Technology*, vol. 29, no. 18, pp. 2663–2669, Jun. 2011.

[4] E. Zedini, I. S. Ansari, and M.-S. Alouini, "Performance analysis of mixed Nakagami-m and Gamma-Gamma dual-hop FSO transmission systems," *IEEE Photonics Journal*, vol. 7, no. 1, pp. 1–20, Feb. 2015.

[5] Q. Gao, R. Wang, Z. Xu, and Y. Hua, "DC-informative joint color-frequency modulation for visible light communications," *Journal of Lightwave Technology*, vol. 33, no. 11, pp. 2181–2188, June 2015.

[6] H. Elgala, R. Mesleh, and H. Haas, "Indoor optical wireless communication: Potential and state-of-the-art," *IEEE Comm. Magazine*, vol. 49, no. 9, pp. 56–62, Sep. 2011.

[7] A. García-Zambrana, C. Castillo-Vázquez, and B. Castillo-Vázquez, "On the capacity of FSO links over Gamma-Gamma atmospheric turbulence channels using OOK signaling," *EURASIP J. Wirel. Commun. Netw.*, vol. 2010, no. 64, pp. 1–11, Jan 2010.

[8] S. Arnon, J. Barry, G. Karagiannidis, R. Schober, and M. Uysal, Eds., *Advanced Optical Wireless Communication Systems*. Cambridge University Press, 2012.

[9] M. A. Khalighi and M. Uysal, "Survey on free space optical communications: A communication theory perspective," *IEEE Communication Surveys and Tutorials*, vol. 16, no. 4, pp. 2231–2258, 4th quarter 2014.

[10] O. E. DeLange, "Optical heterodyne detection," *IEEE Spectrum*, vol. 5, no. 10, pp. 77–85, Oct. 1968.

[11] A. Lapidoth, S. M. Moser, and M. Wigger, "On the capacity of free-space optical intensity channels," *IEEE Trans. on Info. Theory*, vol. 55, no. 10, pp. 4449–4461, Oct. 2009.

[12] A. A. Farid and S. Hranilovic, "Channel capacity and non-uniform signalling for free-space optical intensity channels," *IEEE Journal on Selected Areas in Communications*, vol. 27, no. 9, pp. 1–12, Dec. 2009.

[13] ——, "Capacity bounds for wireless optical intensity channels with Gaussian noise," *IEEE Trans. on Info. Theory*, vol. 56, no. 12, pp. 6066–6077, Dec. 2010.

[14] J.-B. Wang, Q.-S. Hu, J. Wang, M. Chen, and J.-Y. Wang, "Tight bounds on channel capacity for dimmable visible light communications," *Journal of Lightwave Technology*, vol. 31, no. 23, pp. 3771–3779, Dec. 2013.

[15] J.-B. Wang, Q.-S. Hu, J. Wang, M. Chen, Y.-H. Huang, and J.-Y. Wang, "Capacity analysis for dimmable visible light communications," in *Proc. of IEEE International Conference on Communications (ICC)*, Sydney, NSW, June 2014.

[16] T. H. Chan, S. Hranilovic, and F. R. Kschischang, "Capacity-achieving probability measure for conditionally Gaussian channel with bounded input," *IEEE Trans. on Info. Theory*, vol. 51, no. 6, pp. 2073–2088, Jun. 2005.

[17] S. V. Kartalopoulos, *Free Space Optical Networks for Ultra-Broad Band Services*. John Wiley and Sons, Inc., 2011.

[18] M. Berger, *Geometry II*. Springer-Verlag, 1987.

[19] J. M. Morvan, *Generalized Curvatures*. Springer-Verlag, 2008.

[20] D. Cohen-Steiner and J. M. Morvan, "Restricted Delaunay triangulations and normal cycle," in *Proceedings of the Nineteenth Annual Symposium on Computational Geometry (SoCG), A.C.M. Press, New York, NY, USA*, 2003, pp. 312–321.

[21] A. A. Farid and S. Hranilovic, "Outage capacity optimization for free-space optical links with pointing errors," *IEEE/OSA Journal of Lightwave Technology*, vol. 25, no. 7, pp. 1702–1710, Jul. 2007.

[22] H. Kazemi, Z. Mostaani, M. Uysal, and Z. Ghassemlooy, "Outage performance of MIMO FSO systems in Gamma-Gamma fading channels," in *Proc. of IEEE 18th European Conference on Network and Optical Communications*, Graz, Austria, July 2013, pp. 275–280.

[23] M. A. Kashani and M. Uysal, "Outage performance and diversity gain analysis of free-space optical multi-hop parallel relaying," *IEEE/OSA Journal of Optical Communications and Networking*, vol. 5, no. 8, pp. 901–909, Aug. 2013.

[24] A. A. Farid and S. Hranilovic, "Diversity gain and outage probability for MIMO free-space optical links with misalignment," *IEEE Trans. on Communications*, vol. 60, no. 2, pp. 479–487, Feb. 2012.

[25] T. Cover and J. Thomas, *Elements of Information Theory (Second Edition)*. John Wiley and Sons, Inc., 2006.

[26] C. E. Shannon, "Communication in the presence of noise," *Proceedings of the IRE*, vol. 37, no. 1, pp. 10–21, Jan. 1949.

[27] H. AlQuwaiee, I. S. Ansari, and M.-S. Alouini, "On the performance of free-space optical communication systems over double generalized Gamma channel," *IEEE Journal on Selected Areas in Communications*, vol. 33, no. 9, pp. 1829–1840, Sept 2015.

[28] J. M. Wozencraft and I. M. Jacobs, *Principles of Communication Engineering*. John Wiley and Sons, Inc., 1965.

[29] A. Chaaban, J.-M. Morvan, and M.-S. Alouini, "Free-space optical communications: Capacity bounds, approximations, and a new sphere-packing perspective," *KAUST Technical Report http://hdl.handle.net/10754/552096*, Apr. 2015.

[30] S. Rabinowitz, "The volume of an n-simplex with many equal edges," *Missouri Journal of Mathematical Sciences*, vol. 1, pp. 11–17, 1989.

[31] D. Tse and P. Viswanath, *Fundamentals of Wireless Communications*. Cambridge University Press, 2005.

[32] M. K. Simon and M.-S. Alouini, *Digital Communication over Fading Channels*. John Wiley and Sons, Inc., 2005.

[33] M. Abramowitz and I. A. Stegun, *Handbook of Mathematical Functions*. Dover Publications, 1964.

[34] W. Feller, *An Introduction to Probability Theory and its Applications (3rd Edition)*. Wiley, 1968, vol. 1.

[35] S. Li, "Concise formulas for the area and volume of a hyperspherical cap," *Asian Journal of Mathematics and Statistics*, vol. 4, pp. 66–70, Nov. 2010.

Anas Chaaban (S'09 - M'14) received his Maîtrise ès Sciences degree in electronics from the Lebanese University, Lebanon, in 2006. He received his M.Sc. degree in communications technology and his Dr.-Ing. (Ph.D.) degree in Electrical Engineering and Information Technology from the University of Ulm and the Ruhr-University of Bochum, Germany, in 2009 and 2013, respectively. During 2008-2009, he was with the Daimler AG research group on machine vision, Ulm, Germany. He was a Research Assistant with the Emmy- Noether Research Group on Wireless Networks at the University of Ulm, Germany, during 2009-2011, which relocated to Ruhr-Universität Bochum, Germany, in 2011. He was a postdoctoral researcher at the Ruhr-Universität Bochum, Germany, in 2013-2014, and joined King Abdullah University of Science and Technology as a postdoctoral researcher in 2015. He received the best poster award at the IEEE Comm. Theory Workshop in 2011, and the best paper award at ICCSPA in 2015. His research interests are in the areas of information theory and wireless communications.

Jean-Marie Morvan received his PhD from the University Paul Sabatier, Toulouse 3, France. He is a Professor of Mathematics at the University Claude Bernard Lyon 1, France, and a Visiting Professor at King Abdullah University of Science and Technology (KAUST), Saudi Arabia. His main interests are in the field of differential geometry, in particular Riemannian and symplectic geometry, geometric measure theory, application of geometry to different fields such as geology, geophysics, computer graphics, and algorithmic geometry.

Mohamed-Slim Alouini (S'94, M'98, SM'03, F09) was born in Tunis, Tunisia. He received the Ph.D. degree in Electrical Engineering from the California Institute of Technology (Caltech), Pasadena, CA, USA, in 1998. He served as a faculty member in the University of Minnesota, Minneapolis, MN, USA, then in the Texas A&M University at Qatar, Education City, Doha, Qatar before joining King Abdullah University of Science and Technology (KAUST), Thuwal, Makkah Province, Saudi Arabia as a Professor of Electrical Engineering in 2009. His current research interests include the modeling, design, and performance analysis of wireless communication systems.